Toward a Circuit Theory of Communication

Michel T. Ivrlač and Josef A. Nossek, *Fellow, IEEE*

(Invited Paper)

***Abstract*—Electromagnetic field theory provides the *physics* of radio communications, while information theory approaches the problem from a purely *mathematical* point of view. While there is a law of conservation of energy in physics, there is no such law in information theory. Consequently, when, in information theory, reference is made (as it frequently is) to terms like energy, power, noise, or antennas, it is by no means guaranteed that their use is consistent with the physics of the communication system. Circuit theoretic multiport concepts can help in bridging the gap between the physics of electromagnetic fields and the mathematical world of information theory, so that important terms like energy or antenna are indeed used consistently through all layers of abstraction. In this paper, we develop circuit theoretic multiport models for radio communication systems. To demonstrate the utility of the circuit theoretic approach, an in-depth analysis is provided on the impact of impedance matching, antenna mutual coupling, and different sources of noise on the performance of the communication system. Interesting insights are developed about the role of impedance matching and the noise properties of the receive amplifiers, as well as the way array gain and channel capacity scale with the number of antennas in different circumstances. One particularly interesting result is that, with arrays of lossless antennas that receive isotropic background noise, efficient multistreaming can be achieved no matter how densely the antennas are packed.**

***Index Terms*—Antenna losses, channel capacity, circuit theory of communications, impedance matching, multi-input–multi-output (MIMO) systems, physical channel models, receive array gain, transmit array gain.**

I. Introduction

THE ANALYSIS and optimization of communication systems involves a host of technical and scientific disciplines. In the case of radio communications, these include electromagnetic field theory, radio-frequency engineering, and signal, coding, and information theories. The first two disciplines form part of the *physical* theory of communications, for the laws of nature, like the Maxwell equations or the major conservation laws, play a central role in their concepts and methods. In contrast, signal, coding, and information theories are essentially *mathematical* theories. As such, they are not based on the laws of nature but rather on definitions and mathematical logic. Only in conjunction with the physical disciplines can one attempt a complete theory where predictions can be put to the test by experiment. To this end, it is crucial that the mathematical and physical layers of abstraction are consistent with each other.

Manuscript received August 31, 2009; revised December 23, 2009; accepted January 27, 2010. Date of publication April 12, 2010; date of current version July 16, 2010. This paper was recommended by Editor W. A. Serdijn.

The authors are with the Institute for Circuit Theory and Signal Processing, Technische Universität München, 80333 Munich, Germany (e-mail: ivrlac@tum.de; nossek@tum.de).

Digital Object Identifier 10.1109/TCSI.2010.2043994

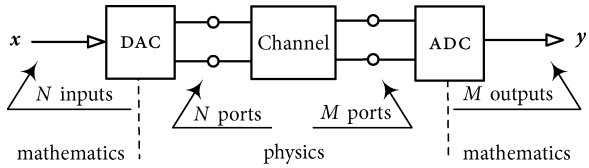

Fig. 1. Abstract model of a communication system showing the domains of physical and mathematical modelings. From the perspective of the latter, it is a vector AWGN channel; from the view point of the former, it is a multiport.

There are several important terms, like "energy," "power," "antenna," "signal," or "noise," which are used in both physical and mathematical disciplines. Yet, from a physics point of view, energy, for instance, is a quantity for which there exists a law of conservation, while in signal and information theories, energy is commonly represented by the squared magnitude of some complex number, for which there *need not* be any law of conservation. Only in the context of wave digital filters [1] is it customary that energy in the signal processing context (called pseudoenergy there) is consistent with physical energy and can be exploited to make sure that the signal processing system is stable. Therefore, special care has to be taken such as to *ensure* that energy in the information theoretic layer of abstraction is consistent with physical energy. To better understand this problem, consider the additive white Gaussian noise (AWGN) channel, shown in Fig. 1, which is popular in information theory and signal processing. For example, a vector $\boldsymbol{x}$ of N signals is presented to the input of the channel, and a vector $\boldsymbol{y}$ of M signals is observed at its output

$$\boldsymbol{y} = \boldsymbol{H}\boldsymbol{x} + \boldsymbol{\vartheta}$$

where the vector $\boldsymbol{\vartheta}$ models an AWGN of a known variance. The transmit power is *defined* to be proportional to the average squared Euclidean norm of $\boldsymbol{x}$ while the $(M \times N)$-dimensional matrix $\boldsymbol{H}$ is called "channel matrix." It got its name due to the fact that once it is known, the information capacity of the AWGN channel can be computed [2]. Hence, from an information theory point of view, the channel matrix tells all about the channel.

The channel input vector $\boldsymbol{x}$ has to be related somehow with a relevant physical quantity of the communication system: perhaps with a voltage or an electric field strength. However, physical power (or energy) cannot be obtained from just one such quantity, but instead, a *conjugated pair* [3] is needed, for example, voltage and electric current, or electric and magnetic field strength. Hence, in a physical description of the channel,

there are twice as many variables (one conjugated pair for each input and each output) than in the information theoretic description. By identifying each conjugated pair with one *port* of an $(M+N)$ port, the noiseless input–output relationship needs an $(M+N)\times(M+N)$ matrix which connects one half of the port variables with the other half [4]. Because $MN < (M+N)^2$, the channel matrix does not have enough degrees of freedom to capture the complete physics of the channel. Yet, from an information theory point of view, it *has to* tell everything about the channel.

Nevertheless, this conflict can be resolved by making use of the *additional* degrees of freedom which come from the relationship between the information theoretic channel input and output on the one hand and some of the physical port variables on the other. By virtue of this relationship, the physical context can be "encoded" into the channel matrix $\boldsymbol{H}$ such that the correct channel capacity can be obtained in the usual way within the information theory layer of abstraction. In Fig. 1, this relationship is represented by the blocks termed DAC (digital-to-analog converter) and ADC (analog-to-digital converter). These terms are used in an abstract sense since it is not merely the technical part of the conversion between the digital and analog domains that takes place, but, more importantly, the conversion between the mathematical and the physical layer of abstraction.

What this conversion looks like depends on how physical quantities (i.e., the conjugated port variables) are related to the mathematical channel inputs and outputs. In the case of radio communication systems, it may appear that electric and magnetic field strengths are natural physical quantities to relate. Indeed, this approach is taken in [5]–[7], where the electromagnetic field equations are brought into a direct contact with information theory. However, this type of approach has the following two major drawbacks. First, field and information theories are not easily united, for both are mature theories which rely on a set of quite different mathematical methods (such as the solution of partial differential equations in continuous space–time on the one hand and statistics and linear algebra on the other). The successful application of such "electromagnetic information theory" requires profound understanding of both theories. The second drawback is related to the treatment of noise. Because classical electromagnetic field theory is a deterministic theory, modeling random noise is difficult. In fact, [5]–[7] have *no* physical noise model. Gaussian random variables just pop up without their relationship with the physical origins of noise or their interaction with the antennas and the receiver (low-noise amplifier and impedance matching network) being made. Because, in information theory, noise is just as important as the signal, the lack of a physical noise model is a serious drawback.

Both the aforementioned problems are solved when the modeling of the physical aspects of communication systems is founded on *circuit theory*. This comes about because of the following three reasons. Regardless of its physical origin, noise is easy to deal with in circuit theory [8]–[11]. In particular, the superposition of contributions of different noise sources (such as amplifier and background noises received by the antennas) directly leads to the important concept of the *noise figure* and its circuit theoretic minimization by *noise matching*. Second, the algebraic mathematical treatment of circuit theoretic multiports interfaces smoothly with signal and information theories. Finally, the complexity of electromagnetic field theory is encapsulated within the multiport model and henceforth does not have to be dealt with directly in signal or information theory. Electromagnetic field theory is therefore confined to the *behavior* of those multiports which model the antennas and propagation aspects of communications. Instead of trying to establish an electromagnetic information theory, we therefore propose to employ a *circuit theory as a medium between the physical world of electrodynamics and the mathematical world of signal and information theories*.

A circuit theoretic approach for modeling communication systems is not new. Wallace and Jensen have used this idea in [12] where they analyze the effect of mutual antenna coupling on channel capacity. We start out with similar ideas as in [12], but with a more rigorous and systematic approach, we are able to actually perform an in-depth analysis of the communication system and obtain some valuable insights. We begin by developing a multiport model for radio communication systems and justify the assumptions that we make on the way. The multiport model covers the physics of signal generation, transmit impedance matching, mutual antenna coupling, receive impedance matching, and noise. For the latter, we distinguish between extrinsic noise that is received by the antennas and intrinsic noise, which originates from the receive amplifiers and their subsequent circuitry.

The N transmit-side and M receive-side antennas, together with the medium that connects the transmitter and receiver, are jointly modeled by one single $(M+N)$ port. Its circuit theoretic description (for example, its scattering or impedance matrix) has to be derived from electromagnetic field theory. Once this is done, the antennas and propagation aspects of communications are completely encapsulated by the multiport such that one does not have to bother with the field equations any longer but can proceed with a much easier multiport matrix description. In this paper, we focus on isotropic antennas that are arranged into uniform linear arrays. With a bare minimum of field theory (essentially using only the concept of the Poynting vector and the law of conservation of energy), we derive in Section III all the necessary properties of the impedance matrix of the antenna multiport.

In Section IV, the developed multiport model is applied to study the impact of impedance matching, mutual antenna coupling, and noise properties on different aspects of communications. As a relevant performance measure, we define the *array gain* in terms of the improvement of the receiver signal-to-noise ratio (SNR) with respect to using only a single antenna at the receiver and the transmitter. Interestingly, it turns out that one has to distinguish between a transmit array gain and a receive array gain, for both are not always identical. We study both array gains in different circumstances and particularly pay attention to how they depend on the number of antennas. It is well known in the antenna and propagation literature [13] that, under certain circumstances, the array gain can grow with the square of the number of antennas. While we confirm this result, we also show that the receive array gain can even grow exponentially with the number of antennas.

Multi-input–multi-output (MIMO) systems are considered in Section V, where the general procedure is developed on how to "encode" the complete physical context into the channel matrix.

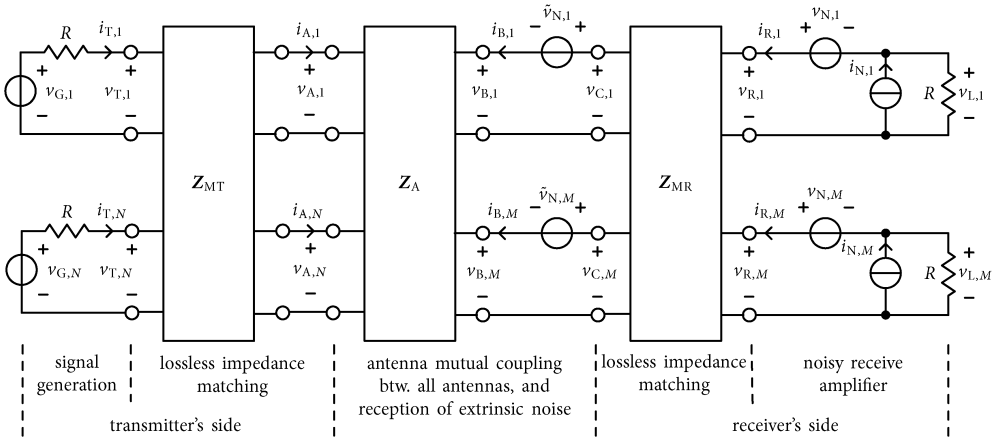

Fig. 2. Linear multiport model of a radio multi-antenna communication system covering signal generation, impedance matching, antenna mutual coupling, and noise of both extrinsic (received by the antennas) and intrinsic (from low-noise amplifiers and remaining circuitry) origins.

By doing so, one makes sure that information theoretic results which are based on this channel matrix are automatically consistent with the physics of the communication system. We demonstrate the power of this approach by analyzing what happens to the channel matrix when the antennas are packed closer and closer. Under certain conditions, the channel matrix can converge to a scaled identity as the antenna separation is reduced toward zero, which shows that efficient multistreaming is possible even with compact arrays.

An analysis of the impact of antenna losses on the array gain and the array efficiency is given alongside a comment on a frequently cited result by Yaru [14]. It turns out that obtaining a high array gain from lossy antennas with a high efficiency is possible provided that the antenna separation and excitation are chosen optimally.

Notation: In the following, we use bold lowercase letters for vectors and bold uppercase letters for matrices. An exception from this rule are bold uppercase letters that are accented by an arrow ($\vec{\cdot}$)—these refer to 3-D field vectors (e.g., electric field). The expectation operation is denoted by $\mathrm{E}[\cdot]$, while *, $^{\mathrm{T}}$, and $^{\mathrm{H}}$, are the complex conjugate, the transposition, and the complex conjugate transposition, respectively. Moreover, $\|\cdot\|_{\mathrm{F}}$ denotes the Frobenius norm, and $\mathbf{I}_n$ and $\mathbf{O}_{m\times n}$ are the n-dimensional identity matrix and the $m \times n$ zero matrix, respectively.

II. Multiport System Model

The physical modeling of multi-antenna radio communication systems which is founded on the circuit theoretic concept of linear multiports is shown in Fig. 2. It consists of four basic parts: *signal generation*, *impedance matching*, *antenna mutual coupling*, and *noise*, which will be discussed in more detail in the following. Before that, however, some general assumptions applied in this paper deserve to be mentioned.

A. Port Variables, Bandwidth, and Power

Complex voltage (v) and current (i) envelopes serve as port variables. The associated real-valued bandpass signals are sufficiently *narrow in bandwidth* compared with the center frequency such that the term

$$\lim_{T\to\infty}\frac{1}{2T}\int_{-T}^{T}\mathrm{Re}\left\{v^*(t)i(t)\right\}\mathrm{d}t$$

is (in a very good approximation) the *average active power* P, which flows into the port. Interpreting v and i, as information carrying, and hence, random signals, we have

$$P=\mathrm{E}\left[\mathrm{Re}\{v^*i\}\right] \tag{1}$$

provided that the time average can be replaced by the ensemble average (which we assume to be the case). The bandwidth shall also be small enough such that the multiports are described by their network properties evaluated at the center frequency.

B. Signal Generation

In the multiport model shown in Fig. 2, the number of antennas at the transmit side is denoted by $N \geq 1$. The generation of the physical signal that is to be transmitted is modeled by N voltage sources which are connected in series with resistances $R > 0$. The ith voltage source is described by its complex voltage envelope $v_{\mathrm{G},i}$, where $i \in \{1, 2, \ldots, N\}$. The maximum average power that can be delivered by the ith generator equals $(1/4)\mathrm{E}[|v_{\mathrm{G},i}|^2]/R$.

C. Impedance Matching Networks

It can be advantageous to use impedance matching networks as a medium between the antenna array and the amplifiers or signal generators. These matching networks can be designed to ensure that the available power of the signal generators is delivered into the antennas (*power matching*) or that the SNR at the outputs of the receive amplifiers is as large as it can be (*noise matching*, [8], [9]) or any other goal one desires [15]. The transmitter-side impedance matching network is modeled as a linear $2N$ port, described by its impedance matrix $\boldsymbol{Z}_{\mathrm{MT}} \in \mathbb{C}^{(2N)\times(2N)}\ .\ \Omega$

$$\begin{bmatrix}\boldsymbol{v}_{\mathrm{T}}\\ \boldsymbol{v}_{\mathrm{A}}\end{bmatrix}=\begin{bmatrix}\boldsymbol{Z}_{\mathrm{MT11}} & \boldsymbol{Z}_{\mathrm{MT12}}\\ \boldsymbol{Z}_{\mathrm{MT21}} & \boldsymbol{Z}_{\mathrm{MT22}}\end{bmatrix}\begin{bmatrix}\boldsymbol{i}_{\mathrm{T}}\\ -\boldsymbol{i}_{\mathrm{A}}\end{bmatrix} \tag{2}$$

displayed and partitioned into four square matrices. We introduce vectors $\boldsymbol{v}_{\mathrm{T}} = [v_{\mathrm{T},1}\ v_{\mathrm{T},2}\ \ldots\ v_{\mathrm{T},N}]^{\mathrm{T}}$ and $\boldsymbol{i}_{\mathrm{T}} = [i_{\mathrm{T},1}\ i_{\mathrm{T},2}\ \ldots\ i_{\mathrm{T},N}]^{\mathrm{T}}$ and the corresponding vectors $\boldsymbol{v}_{\mathrm{A}} \in \mathbb{C}^{N\times 1}\cdot\mathrm{V}$ and $-\boldsymbol{i}_{\mathrm{A}} \in \mathbb{C}^{N\times 1}\cdot\mathrm{A}$ for the ports connecting to the transmit antenna array. In a similar way, the receiver-side impedance matching network is modeled as a linear $2M$ port and described by its impedance matrix $\boldsymbol{Z}_{\mathrm{MR}} \in \mathbb{C}^{(2M)\times(2M)}\cdot\Omega$

$$\begin{bmatrix}\boldsymbol{v}_{\mathrm{R}}\\ \boldsymbol{v}_{\mathrm{C}}\end{bmatrix} = \begin{bmatrix}\boldsymbol{Z}_{\mathrm{MR11}} & \boldsymbol{Z}_{\mathrm{MR12}}\\ \boldsymbol{Z}_{\mathrm{MR21}} & \boldsymbol{Z}_{\mathrm{MR22}}\end{bmatrix}\begin{bmatrix}\boldsymbol{i}_{\mathrm{R}}\\ -\boldsymbol{i}_{\mathrm{B}}\end{bmatrix} \tag{3}$$

where $\boldsymbol{Z}_{\mathrm{MR}}$ is partitioned into four square matrices. The vectors of voltage and current envelopes, i.e., $\boldsymbol{v}_{\mathrm{R}}, \boldsymbol{v}_{\mathrm{C}} \in \mathbb{C}^{M\times 1}\cdot\mathrm{V}$ and $\boldsymbol{i}_{\mathrm{R}}, \boldsymbol{i}_{\mathrm{B}} \in \mathbb{C}^{M\times 1}\cdot\mathrm{A}$, are defined analogously to the case of transmit impedance matching and are shown in Fig. 2. Herein, $M \geq 1$ denotes the number of antennas at the receiver. We will treat the impedance matching networks as *lossless* and *reciprocal* multiports. Note that the lack of dissipation causes them to be *noiseless*, too [16]. Describing lossless and reciprocal multiports $\boldsymbol{Z}_{\mathrm{MT}}$ and $\boldsymbol{Z}_{\mathrm{MR}}$ must be *symmetric matrices with vanishing real parts* [17]. We assume that the amplifiers are unconditionally stable such that they remain stable with any lossless matching networks.

D. Antenna Mutual Coupling

Let the antennas at the transmit end of the link be enumerated by the integers from 1 to N and the remaining antennas by the integers from $N+1$ to $N+M$. Assume that the antennas are made of wires and that an electric current flows through antenna k. Suppose we can arrange things such that *no* currents flow through the remaining antennas. Because the antennas interact, voltages appear across all antenna wires. The ratio of the complex envelope of the voltage observed at the jth antenna to the complex envelope of the excitation current applied to the kth antenna is then the mutual coupling coefficient between the kth and the jth antenna. As (k, j) ranges over all possible combinations, we obtain all $(M+N)^2$ coupling coefficients which are clearly the entries of the impedance matrix $\boldsymbol{Z}_{\mathrm{A}} \in \mathbb{C}^{(M+N)\times(M+N)}\cdot\Omega$, which describes a linear $(M+N)$ port. By associating the antenna currents and voltages by port currents and voltages, the following multiport model is obtained:

$$\begin{bmatrix}\boldsymbol{v}_{\mathrm{A}}\\ \boldsymbol{v}_{\mathrm{B}}\end{bmatrix} = \begin{bmatrix}\boldsymbol{Z}_{\mathrm{AT}} & \boldsymbol{Z}_{\mathrm{ATR}}\\ \boldsymbol{Z}_{\mathrm{ART}} & \boldsymbol{Z}_{\mathrm{AR}}\end{bmatrix}\begin{bmatrix}\boldsymbol{i}_{\mathrm{A}}\\ \boldsymbol{i}_{\mathrm{B}}\end{bmatrix} \tag{4}$$

where $\boldsymbol{Z}_{\mathrm{A}}$ is partitioned into four blocks: transmit and receive impedance matrices $\boldsymbol{Z}_{\mathrm{AT}} \in \mathbb{C}^{N\times N}\cdot\Omega$ and $\boldsymbol{Z}_{\mathrm{AR}} \in \mathbb{C}^{M\times M}\cdot\Omega$, respectively, and the two transimpedance matrices $\boldsymbol{Z}_{\mathrm{ART}} \in \mathbb{C}^{M\times N}\cdot\Omega$ and $\boldsymbol{Z}_{\mathrm{ATR}} \in \mathbb{C}^{N\times M}\cdot\Omega$. Because antennas are reciprocal [18], we have $\boldsymbol{Z}_{\mathrm{AT}} = \boldsymbol{Z}_{\mathrm{AT}}^{\mathrm{T}}$, $\boldsymbol{Z}_{\mathrm{AR}} = \boldsymbol{Z}_{\mathrm{AR}}^{\mathrm{T}}$, and $\boldsymbol{Z}_{\mathrm{ATR}} = \boldsymbol{Z}_{\mathrm{ART}}^{\mathrm{T}}$.

Even though it would be impossible to establish zero port currents in a real experiment, all we have to do to deduce the impedance matrix from theory is to calculate what the port voltages are *supposed to be* if all port currents, except one, *happened to be* zero. This is comparatively easy—at least for thin-wire antennas. A vanishing electric current in the antenna wire means that the antenna does not alter the electromagnetic field [19], becoming essentially "invisible." Assuming this so-called *canonical minimum-scattering* [20] property, *the coefficients of the impedance matrix can be computed by just looking at pairs of antennas without having to consider the neighbors, since they do not interfere for zero current*.

E. Noise

In radio communication systems, it makes sense to distinguish between *intrinsic* noise and *extrinsic* noise. The latter comes from background radiation which is received by the antennas. While there are numerous origins of background noise [21], we can always model it by the inclusion of M voltage sources with complex voltage envelopes $\tilde{v}_{N,j}$, where $j \in \{1, 2, \ldots, M\}$, as shown in Fig. 2. These $\tilde{v}_{N,j}$'s are the complex envelopes of the noise voltages that appear at the antenna ports when no currents flow (open-circuit noise voltages).

The reader may have noticed that, in Fig. 2, noise voltage sources are included only at the receiver's ports. Strictly speaking, one has to have another set of N noise voltage sources in series with the transmit-side ports. However, they are omitted here because of the following argument. In radio communications, one usually encounters a strong attenuation as the signal propagates from the transmitter to the receiver. Consequently, the transmit power or the associated voltage and current amplitudes are much larger with respect to the noise we observe in practice.

The complex voltage envelopes $\tilde{v}_{\mathrm{N},j}$ and $\tilde{v}_{\mathrm{N},k}$ are usually correlated. This is modeled by the covariance matrix

$$\boldsymbol{\phi} = \frac{1}{\tilde{\beta}R_{\mathrm{r}}^2}\mathrm{E}\left[\tilde{\boldsymbol{v}}_{\mathrm{N}}\tilde{\boldsymbol{v}}_{\mathrm{N}}^{\mathrm{H}}\right] \tag{5}$$

where $\tilde{\boldsymbol{v}}_{\mathrm{N}} = [\tilde{v}_{\mathrm{N},1}\ \tilde{v}_{\mathrm{N},2}\ \ldots\ \tilde{v}_{\mathrm{N},M}]^{\mathrm{T}}$. The symbol R_{r} denotes the so-called *radiation resistance* of the antennas

$$R_{\mathrm{r}} = \mathrm{Re}\left\{(\boldsymbol{Z}_{\mathrm{AR}})_{j,j}\right\} \qquad \forall j. \tag{6}$$

It is standard practice to write

$$\tilde{\beta} = \frac{4\mathrm{k}T_{\mathrm{A}}\Delta f}{R_{\mathrm{r}}} \tag{7}$$

wherein k denotes the Boltzmann constant, while Δf is the bandwidth of the desired signals, which we assume is small enough such that the noise power density can be considered constant within this band of frequencies. The term T_{A} is the so-called *noise temperature* of the antennas. It is the absolute temperature that a resistor with resistance R_{r} has to have such that it generates an open-circuit thermal noise voltage of variance $\tilde{\beta}R_{\mathrm{r}}^2$ [11]. By requiring that

$$(\boldsymbol{\phi})_{j,j} = 1 \quad \forall j \tag{8}$$

it follows that, for the mean square open-circuit noise voltage

$$\mathrm{E}\left[|\tilde{v}_{\mathrm{N},j}|^2\right] = \tilde{\beta}R_{\mathrm{r}}^2 = 4\mathrm{k}T_{\mathrm{A}}R_{\mathrm{r}}\Delta f. \tag{9}$$

In this way, the noisy antennas behave as if the received background noise was generated by their radiation resistance at temperature T_{A}.

The *intrinsic* noise originates from the components that are connected to the other end of the receiver impedance matching network. Most of the noise stems from the first stage of the low-noise amplifier, but other circuit components, including the ADC, contribute, too. When we model the low-noise amplifier and all the subsequent circuitry as a two port, we need two noise

sources to describe its noise properties—one source per port or, equivalently, two noise sources at the input [10], as shown in Fig. 2 in the form of M noise voltage sources with the complex voltage envelopes $v_{\mathrm{N},j}$ and M noise current sources with the complex current envelopes $i_{\mathrm{N},j}$, where $j \in \{1,2,\ldots,M\}$. For simplicity, the input impedances of the low-noise amplifiers are assumed to be real valued and equal to R. We write for the statistical properties of the intrinsic noise sources

$$\left.\begin{aligned} \mathrm{E}\left[\boldsymbol{i}_{\mathrm{N}}\boldsymbol{i}_{\mathrm{N}}^{\mathrm{H}}\right] &= \beta\mathbf{I}_M \\ \mathrm{E}\left[\boldsymbol{v}_{\mathrm{N}}\boldsymbol{v}_{\mathrm{N}}^{\mathrm{H}}\right] &= \beta R_{\mathrm{N}}^2\mathbf{I}_M \\ \mathrm{E}\left[\boldsymbol{v}_{\mathrm{N}}\boldsymbol{i}_{\mathrm{N}}^{\mathrm{H}}\right] &= \rho\beta R_{\mathrm{N}}\mathbf{I}_M. \end{aligned}\right\} \tag{10}$$

The fact that all covariance matrices are diagonal reflects the reasonable assumption that the *physical* noise sources in each of the low-noise amplifiers (and the subsequent circuitry) are independent with respect to different amplifiers (and their subsequent circuitry). The idea that all three covariance matrices are even scaled identities means that we assumed the statistical properties to be the same for each amplifier, which is reasonable. From the first and second lines of (10), we see that

$$R_{\mathrm{N}} = \sqrt{E\left[|v_{\mathrm{N},j}|^2\right]/E\left[|i_{\mathrm{N},j}|^2\right]} \quad \forall j \tag{11}$$

is the so-called *noise resistance*. The complex noise voltage envelope $v_{\mathrm{N},j}$ and the complex noise current envelope $i_{\mathrm{N},j}$ belonging to the same amplifier are usually correlated. From (11) and the first and last lines of (10), we see that

$$\rho = \frac{E\left[v_{\mathrm{N},j}i_{\mathrm{N},j}^*\right]}{\sqrt{E\left[|v_{\mathrm{N},j}|^2\right]\cdot E\left[|i_{\mathrm{N},j}|^2\right]}} \quad \forall j \tag{12}$$

is the *complex noise correlation coefficient*.

F. Unilateral Approximation

Because antennas are reciprocal [18], it is generally true that, in (4), $\boldsymbol{Z}_{\mathrm{ATR}} = \boldsymbol{Z}_{\mathrm{ART}}^{\mathrm{T}}$. However, it is also true that the signal attenuation between the transmitter and the receiver is usually extremely large. Hence, $\|\boldsymbol{Z}_{\mathrm{ATR}}\|_{\mathrm{F}} = \|\boldsymbol{Z}_{\mathrm{ART}}\|_{\mathrm{F}} \ll \|\boldsymbol{Z}_{\mathrm{AT}}\|_{\mathrm{F}}$ holds true in practice. This motivates us to keep $\boldsymbol{Z}_{\mathrm{ART}}$ as is, but to set $\boldsymbol{Z}_{\mathrm{ATR}} = \mathbf{O}_{N\times M}$ in (4):

$$\begin{bmatrix}\boldsymbol{v}_{\mathrm{A}}\\ \boldsymbol{v}_{\mathrm{B}}\end{bmatrix} \approx \begin{bmatrix}\boldsymbol{Z}_{\mathrm{AT}} & \mathbf{O}_{N\times M}\\ \boldsymbol{Z}_{\mathrm{ART}} & \boldsymbol{Z}_{\mathrm{AR}}\end{bmatrix}\begin{bmatrix}\boldsymbol{i}_{\mathrm{A}}\\ \boldsymbol{i}_{\mathrm{B}}\end{bmatrix}. \tag{13}$$

The expression (13) will be called the *unilateral approximation*. Because $\boldsymbol{v}_{\mathrm{A}} \approx \boldsymbol{Z}_{\mathrm{AT}}\boldsymbol{i}_{\mathrm{A}}$, the electrical properties at the transmit-side antenna ports are (almost) independent of what happens at the receiver. This significantly simplifies the analysis of the communication system and synthesis of some of its parts (for example, the impedance matching networks). The approximate equality in (13) becomes an almost exact one, provided that $\|\boldsymbol{Z}_{\mathrm{ART}}\|_{\mathrm{F}}$ is small enough. It can be shown (see Appendix A) that

$$\|\boldsymbol{Z}_{\mathrm{ART}}\|_{\mathrm{F}} \ll \sqrt{\frac{\xi\xi'}{MN}} \tag{14}$$

is sufficiently small in practice. Herein, ξ and ξ' denote the *smallest eigenvalues* of $\mathrm{Re}\{\boldsymbol{Z}_{\mathrm{AT}}\}$ and $\mathrm{Re}\{\boldsymbol{Z}_{\mathrm{AR}}\}$, respectively. Because $\|\boldsymbol{Z}_{\mathrm{ART}}\|_{\mathrm{F}}$ is proportional to the $\sqrt{MN}$ and inversely proportional to the distance D between the transmitter and receiver, we have to ensure that the distance D is large compared with some critical distance D_{crit}, where

$$D_{\mathrm{crit}} \propto \frac{MN}{\sqrt{\xi\xi'}}. \tag{15}$$

The values ξ and ξ' depend on the number of antennas, their radiation pattern, and—most importantly—the separation d between neighboring antennas in the arrays. It will be shown that ξ or ξ' decrease toward zero as the antennas are placed closer and closer within the transmit- or receive-side array, respectively. This means that when compact antenna arrays are used at either side of the link, the critical distance D_{crit} between the receiver and the transmitter is larger than when the antennas are widely spaced. This is in accordance with a result obtainable from electromagnetic field theory, which states that the near field of an antenna array increases its size unboundedly as the antennas inside the array are placed closer and closer to each other [22]. *In this paper, it is assumed that the receiver and the transmitter are separated far enough such that* (14) *holds true and the unilateral approximation* (13) *can be used.*

G. Input–Output Relationship

We put all complex envelopes $v_{\mathrm{L},k}$, with $k \in \{1,2,\ldots M\}$, that appear at the system's output (see Fig. 2) into the vector $\boldsymbol{v}_{\mathrm{L}} \in \mathbb{C}^{M\times 1}\cdot\mathrm{V}$. Because the circuit from Fig. 2 is linear, the relationship between $\boldsymbol{v}_{\mathrm{L}}$ and the complex envelopes of the voltages and currents generated by the signal and noise sources can, in general, be written as

$$\boldsymbol{v}_{\mathrm{L}} = \boldsymbol{D}\boldsymbol{v}_{\mathrm{G}} + \sqrt{R}\boldsymbol{\eta} \tag{16}$$

where $\boldsymbol{\eta} \in \mathbb{C}^{M\times 1}\cdot\sqrt{\mathrm{W}}$ is the contribution of the noise sources. Scaling by $\sqrt{R}$ is performed such that $\|\boldsymbol{\eta}\|_2^2$ has the physical dimension of *power*. Using the unilateral approximation, we obtain from circuit analysis

$$\boldsymbol{D} = \boldsymbol{Q}\boldsymbol{Z}_{\mathrm{RT}}(R\mathbf{I}_N + \boldsymbol{Z}_{\mathrm{T}})^{-1} \tag{17}$$

$$\boldsymbol{\eta} = \frac{1}{\sqrt{R}}\boldsymbol{Q}(\boldsymbol{Z}_{\mathrm{R}}\boldsymbol{i}_{\mathrm{N}} - \boldsymbol{v}_{\mathrm{N}} + \boldsymbol{F}_{\mathrm{R}}\tilde{\boldsymbol{v}}_{\mathrm{N}}) \tag{18}$$

where we have introduced the impedance matrices

$$\left.\begin{aligned} \boldsymbol{Z}_{\mathrm{R}} &= \boldsymbol{Z}_{\mathrm{MR11}} - \boldsymbol{F}_{\mathrm{R}}\boldsymbol{Z}_{\mathrm{MR21}} \\ \boldsymbol{Z}_{\mathrm{T}} &= \boldsymbol{Z}_{\mathrm{MT11}} - \boldsymbol{F}_{\mathrm{T}}\boldsymbol{Z}_{\mathrm{MT21}} \\ \boldsymbol{Z}_{\mathrm{RT}} &= \boldsymbol{F}_{\mathrm{R}}\boldsymbol{Z}_{\mathrm{ART}}\boldsymbol{F}_{\mathrm{T}}^{\mathrm{T}} \end{aligned}\right\} \tag{19}$$

and defined the abbreviations

$$\left.\begin{aligned} \boldsymbol{F}_{\mathrm{R}} &= \boldsymbol{Z}_{\mathrm{MR12}}(\boldsymbol{Z}_{\mathrm{MR22}} + \boldsymbol{Z}_{\mathrm{AR}})^{-1} \\ \boldsymbol{F}_{\mathrm{T}} &= \boldsymbol{Z}_{\mathrm{MT12}}(\boldsymbol{Z}_{\mathrm{MT22}} + \boldsymbol{Z}_{\mathrm{AT}})^{-1} \\ \boldsymbol{Q} &= R(R\mathbf{I}_M + \boldsymbol{Z}_{\mathrm{R}})^{-1} \end{aligned}\right\} \tag{20}$$

for notational convenience. Notice that the system composed of the multi-antenna multiport and the two impedance matching networks is described in the noise-free case by

$$\left.\begin{bmatrix}\boldsymbol{v}_{\mathrm{T}}\\ \boldsymbol{v}_{\mathrm{R}}\end{bmatrix}\right|_{\tilde{\boldsymbol{v}}_{\mathrm{N}}=\mathbf{0}} = \begin{bmatrix}\boldsymbol{Z}_{\mathrm{T}} & \mathbf{O}_{N\times M}\\ \boldsymbol{Z}_{\mathrm{RT}} & \boldsymbol{Z}_{\mathrm{R}}\end{bmatrix}\begin{bmatrix}\boldsymbol{i}_{\mathrm{T}}\\ \boldsymbol{i}_{\mathrm{R}}\end{bmatrix} \tag{21}$$

which is true within the realm of the unilateral approximation. This shows the circuit theoretic meaning of $\boldsymbol{Z}_{\mathrm{R}}$, $\boldsymbol{Z}_{\mathrm{T}}$, and $\boldsymbol{Z}_{\mathrm{RT}}$.

H. Transmit Power and Noise Covariance

The *transmit power* is defined

$$P_{\mathrm{Tx}} = \mathrm{E}\left[\mathrm{Re}\left\{\boldsymbol{v}_{\mathrm{T}}^{\mathrm{H}}\boldsymbol{i}_{\mathrm{T}}\right\}\right] \tag{22}$$

$$= \mathrm{E}\left[\mathrm{Re}\left\{\boldsymbol{v}_{\mathrm{A}}^{\mathrm{H}}\boldsymbol{i}_{\mathrm{A}}\right\}\right] \tag{22a}$$

as the sum of the average active powers that flow into the N ports at the transmitter side of the matched multiport system. As the matching networks are lossless, the so-defined transmit power is also equal to the average active power that flows into the transmit antenna array. *Assuming lossless antennas, the transmit power is also equal to the radiated power* P_{rad}. We will come back to this important point later on. From (21), we have $\boldsymbol{v}_{\mathrm{T}} = \boldsymbol{Z}_{\mathrm{T}}\boldsymbol{i}_{\mathrm{T}}$, and $\boldsymbol{Z}_{\mathrm{T}}^{\mathrm{H}} = \boldsymbol{Z}_{\mathrm{T}}^{*}$ holds true because of reciprocity (recall from Section II-C that the matching networks are reciprocal such that the cascade of matching networks and multi-antenna multiport is reciprocal). As $\boldsymbol{v}_{\mathrm{T}} = \boldsymbol{v}_{\mathrm{G}} - R\boldsymbol{i}_{\mathrm{T}}$

$$P_{\mathrm{Tx}} = \frac{1}{4R}\mathrm{E}\left[\boldsymbol{v}_{\mathrm{G}}^{\mathrm{H}}\boldsymbol{B}\boldsymbol{v}_{\mathrm{G}}\right] \tag{23}$$

with the "power-coupling" matrix

$$\boldsymbol{B} = 4R\left(R\mathbf{I}_{\mathrm{N}} + \boldsymbol{Z}_{\mathrm{T}}^{*}\right)^{-1}\mathrm{Re}\{\boldsymbol{Z}_{\mathrm{T}}\}\left(R\mathbf{I}_{N} + \boldsymbol{Z}_{\mathrm{T}}\right)^{-1} \tag{24}$$

for which $\boldsymbol{B} = \boldsymbol{B}^{\mathrm{H}} > \mathbf{0}$ holds true, because the transmit power is positive for any $\boldsymbol{v}_{\mathrm{G}} \neq \mathbf{0}$. The noise covariance is defined as

$$\boldsymbol{R}_{\boldsymbol{\eta}} = \mathrm{E}[\boldsymbol{\eta}\boldsymbol{\eta}^{\mathrm{H}}] \in \mathbb{C}^{M\times M}\cdot\mathrm{W}. \tag{25}$$

With (5), (10), and (18), we obtain

$$\boldsymbol{R}_{\boldsymbol{\eta}} = \frac{\beta R_{\mathrm{r}}^{2}}{R}\boldsymbol{Q}\boldsymbol{\Upsilon}\boldsymbol{Q}^{\mathrm{H}} \tag{26}$$

where the dimensionless matrix $\boldsymbol{\upsilon} \in \mathbb{C}^{M\times M}$ is defined as

$$\boldsymbol{\Upsilon} = \frac{1}{R_{\mathrm{r}}^{2}}\boldsymbol{Z}_{\mathrm{R}}\boldsymbol{Z}_{\mathrm{R}}^{*} - \frac{2R_{\mathrm{N}}}{R_{\mathrm{r}}^{2}}\mathrm{Re}\{\rho^{*}\boldsymbol{Z}_{\mathrm{R}}\} + \frac{R_{\mathrm{N}}^{2}}{R_{\mathrm{r}}^{2}}\mathbf{I}_{M} + \frac{\tilde{\beta}}{\beta}\boldsymbol{F}_{\mathrm{R}}\boldsymbol{\phi}\boldsymbol{F}_{\mathrm{R}}^{\mathrm{H}}. \tag{27}$$

III. Multi-Antenna Multiport

Shifting our focus back to the antenna multiport, what can we say about its impedance matrix $\boldsymbol{Z}_{\mathrm{A}}$? Certainly it depends on the type of antennas, their spatial arrangement, the distance between the transmitter and the receiver, and on the medium connecting them. Obviously, this is a complicated problem. In order to handle it here, we shall restrict the discussion to simple antennas in simple arrangements with a simple medium, yet complex enough such that the important physical effects of multi-antenna communications are visible.

The Hertzian dipole may come into mind when searching for a "simple" antenna. Nevertheless, the authors prefer yet a simpler approach: the *isotropic* antenna. This concept enjoys extreme popularity in the literature of array signal processing and information theory (e.g., [23]–[27]), obviously because of its inherent simplicity. The only trouble is that isotropic electrodynamic vector fields do not exist [18]. The reason for this is that the isotropic vector field, far enough removed from the antenna, is *not* supposed to change when we turn the antenna in *any* direction. Only radially symmetric vector fields fulfill such a requirement. However, radial symmetry causes the curl of a vector to be zero, such that the Maxwell equations permit radially symmetric fields in free space only for the *static* case. Nevertheless, the idea of the isotropic antenna can be saved if we do not think *only* in terms of the electric and magnetic field vectors, but in terms of the Poynting vector field which is the cross product of the electric and magnetic field vectors [28]. *The isotropic antenna is defined such that the radial component of the Poynting vector is independent of the direction*. Hence, the isotropic antenna shall be isotropic with respect to the radiated power density instead of electric or magnetic field vectors. This is permitted by the Maxwell equations.

With the additional assumption that the isotropic antennas are lossless, one can find $\mathrm{Re}\{\boldsymbol{Z}_{\mathrm{AT}}\}$ and $\mathrm{Re}\{\boldsymbol{Z}_{\mathrm{AR}}\}$ just from the law of conservation of energy. Later, it will become clear that the real part is all one needs to know about $\boldsymbol{Z}_{\mathrm{AT}}$ and $\boldsymbol{Z}_{\mathrm{AR}}$ regarding the *analysis* of a matched multi-antenna system. Hence, this is good news. Furthermore, the real part of the impedance matrix of a linear array of isotropic antennas is qualitatively the same as one would obtain for a linear array of Hertzian dipoles [29]. This shows that the concept of isotropic antennas, albeit simple, does capture the essential physics of mutual near-field coupling.

A. Radiated Power

In order to calculate the real part of the impedance matrix of an array of isotropic antennas, let us first take a look into the behavior of "ordinary" antennas. We can compute the power P_{rad} which is radiated by an ordinary antenna in free space by integrating the Poynting vector over any closed surface ∂V which completely surrounds the antenna [30]. With the vectors $\vec{\boldsymbol{E}}$ and $\vec{\boldsymbol{H}}$ of the complex envelopes of the electric and magnetic fields, this becomes

$$P_{\mathrm{rad}} = \int_{\partial V}\mathrm{E}\left[\mathrm{Re}\{\vec{\boldsymbol{E}}^{*}\times\vec{\boldsymbol{H}}\}\right]\mathrm{d}\vec{\boldsymbol{A}}. \tag{28}$$

By placing the antenna in the origin of a spherical coordinate system (see left-hand side of Fig. 3) and choosing for ∂V the surface of a sphere of radius r centered in the origin, we can express the radiated power as

$$P_{\mathrm{rad}} = \int_{0}^{2\pi}\int_{0}^{\pi}\mathrm{E}\left[\mathrm{Re}\left\{E_{\theta}^{*}H_{\phi} - E_{\phi}^{*}H_{\theta}\right\}\right]r^{2}\sin(\theta)\mathrm{d}\theta\mathrm{d}\phi. \tag{29}$$

Let r be large enough such that the surface of the sphere is inside the far field of the antenna; then, the electromagnetic field is a spherical transversal electric wave [18]

$$\begin{bmatrix}E_r & E_\theta & E_\phi\end{bmatrix} = \frac{\mathrm{e}^{-\mathrm{j}kr}}{r}\begin{bmatrix}0 & F_\theta(\theta,\phi) & F_\phi(\theta,\phi)\end{bmatrix} \tag{30}$$

wherein $k = 2\pi/\lambda$ is the wavenumber, λ is the wavelength, and F_θ and F_ϕ are functions specific to the antenna used. The empty-space Maxwell equation $\vec{\boldsymbol{H}} = (\mathrm{j}/\omega m_0)\boldsymbol{\nabla}\times\vec{\boldsymbol{E}}$ used in (30), with $\mu_0 = 4\pi\times10^{-7}\ \mathrm{H/m}$ and the angular frequency ω, requires that $H_\theta = -E_\phi/Z_0$ and $H_\phi = E_\theta/Z_0$, where $Z_0 = m_0 c \approx 377\ \Omega$ and c is the speed of light. Hence, (29) becomes

$$P_{\mathrm{rad}} = \frac{1}{Z_0}\int_{0}^{2\pi}\int_{0}^{\pi}\mathrm{E}\left[|E|^{2}\right]r^{2}\sin(\theta)\mathrm{d}\theta\mathrm{d}\phi \tag{31}$$

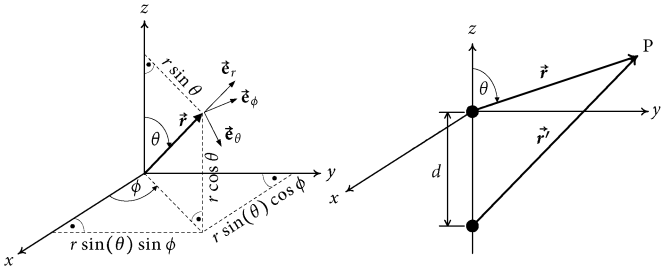

Fig. 3. (Left) Definition of the spherical coordinate system. (Right) Array of two antennas and a point P in the far field.

where $|E|^2 = \|\vec{\boldsymbol{E}}\|_2^2 = |E_\theta|^2 + |E_\phi|^2$ is the intensity of the electric field. Let us write (30) as

$$\vec{\boldsymbol{E}} = \tilde{\alpha}(\theta,\phi)\cdot\frac{\mathrm{e}^{-\mathrm{j}kr}}{r}\cdot\vec{\mathbf{e}}_{\mathbf{0}}(\theta,\phi), \qquad \vec{\mathbf{e}}_0\cdot\vec{\boldsymbol{r}} = 0 \tag{32}$$

where $\vec{\mathbf{e}}_{\mathbf{0}}$ is a unit vector pointing in the direction of the electric far field and

$$\tilde{\alpha}(\theta,\phi) = \frac{F_\theta(\theta,\phi)}{\vec{\mathbf{e}}_0\cdot\vec{\mathbf{e}}_\theta} = \frac{F_\phi(\theta,\phi)}{\vec{\mathbf{e}}_0\cdot\vec{\mathbf{e}}_\phi}.$$

Because $\vec{\mathbf{e}}_{\mathbf{0}}$ is a unity vector, one can see by taking the magnitude of (32) that $|\tilde{\alpha}(\theta,\phi)|^2 = r^2|E|^2$. Since (31) does not depend on $\vec{\mathbf{e}}_0$, we do not need to know where the electric field vector is pointing. We just look at its magnitude

$$P_{\mathrm{rad}} = \frac{1}{Z_0}\int_0^{2\pi}\int_0^{\pi}\mathrm{E}\left[|\tilde{\alpha}(\theta,\phi)|^2\right]\sin(\theta)\mathrm{d}\theta\mathrm{d}\phi. \tag{33}$$

B. Array Impedance Matrix

Consider two identical antennas, one located in the origin, as before, and another one which is displaced by the distance d along the negative z-axis, as shown in the right-hand side of Fig. 3. The electric field at a point P, far away from the antennas, can be written as the linear superposition $\vec{\boldsymbol{E}} = \vec{\boldsymbol{E}}_1 + \vec{\boldsymbol{E}}_2$. The electric fields generated by each antenna

$$\left.\begin{aligned}\vec{\boldsymbol{E}}_1 &= \alpha_1(\theta,\phi)\cdot\frac{\mathrm{e}^{-\mathrm{j}kr}}{r}\cdot\vec{\mathbf{e}}_{0,1}(\theta,\phi)\\ \vec{\boldsymbol{E}}_2 &= \alpha_2(\theta,\phi)\cdot\frac{\mathrm{e}^{-\mathrm{j}kr'}}{r'}\cdot\vec{\mathbf{e}}_{0,2}(\theta,\phi)\end{aligned}\right\} \tag{34}$$

where r and r' are the distances between the point P and the first and the second antenna, respectively (see right-hand side of Fig. 3). Now, let these two identical antennas be oriented in the same way and excited by currents of complex envelopes i_1 and i_2, respectively. Then, we have $\vec{\mathbf{e}}_{0,1} = \vec{\mathbf{e}}_{0,2} = \vec{\mathbf{e}}_0$ and

$$\left.\begin{aligned}\alpha_1(\theta,\phi) &= \alpha(\theta,\phi)\cdot i_1\\ \alpha_2(\theta,\phi) &= \alpha(\theta,\phi)\cdot i_2.\end{aligned}\right\} \tag{35}$$

When $i_2 = 0$, the second antenna does not change the field of the first and vice versa (see also the discussion in Section II-D on antenna mutual coupling). Hence, the function $\alpha(\theta,\phi)$ is *not* influenced by the neighboring antenna—it is the same function we would obtain if only one antenna was present in the first place.

The distance r' can be expressed in terms of r and elevation θ (see right-hand side of Fig. 3)

$$r' = r\sqrt{1+\frac{d^2}{r^2}+\frac{2d}{r}\cos\theta} \approx r + d\cos\theta, \qquad r \gg d \tag{36}$$

so that, in a large enough distance $r \gg d$ in the far field, we obtain from $\vec{\boldsymbol{E}} = \vec{\boldsymbol{E}}_1 + \vec{\boldsymbol{E}}_2$, using (34)–(36)

$$\vec{\boldsymbol{E}} = \alpha(\theta,\phi)\frac{\mathrm{e}^{-\mathrm{j}kr}}{r}(i_1 + i_2\mathrm{e}^{-\mathrm{j}kd\cos\theta})\vec{\mathbf{e}}_0(\theta,\phi) \tag{37}$$

$$= \alpha(\theta,\phi)\boldsymbol{a}^{\mathrm{T}}(\theta)\boldsymbol{i}_{\mathrm{A}}\cdot\frac{\mathrm{e}^{-\mathrm{j}kr}}{r}\vec{\mathbf{e}}_0(\theta,\phi) \tag{37a}$$

where we have collected the current envelopes into the vector $\boldsymbol{i}_{\mathrm{A}} = [i_1\ i_2]^{\mathrm{T}}$ and defined the *array steering vector*

$$\boldsymbol{a}(\theta) = \begin{bmatrix}1 & \mathrm{e}^{-\mathrm{j}kd\cos\theta}\end{bmatrix}^{\mathrm{T}}. \tag{38}$$

Comparing (37a) with (32), we see that

$$\tilde{\alpha}(\theta,\phi) = \alpha(\theta,\phi)\cdot\boldsymbol{a}^{\mathrm{T}}(\theta)\boldsymbol{i}_A. \tag{39}$$

Substituting (39) into (33) and pulling the expectation operation outside the integrals, we find

$$P_{\mathrm{rad}} = \mathrm{E}\left[\boldsymbol{i}_{\mathrm{A}}^{\mathrm{H}}\left(Z_0^{-1}\int_0^{2\pi}\int_0^{\pi}|\alpha(\theta,\phi)|^2\,\boldsymbol{a}^*(\theta)\boldsymbol{a}^{\mathrm{T}}(\theta)\sin(\theta)\mathrm{d}\theta\mathrm{d}\phi\right)\boldsymbol{i}_{\mathrm{A}}\right]. \tag{40}$$

On the other hand, the definition of the *transmit power* from (22a) together with $\boldsymbol{v}_{\mathrm{A}} = \boldsymbol{Z}_{\mathrm{AT}}\boldsymbol{i}_{\mathrm{A}}$ from (13) and the relationship $\boldsymbol{Z}_{\mathrm{AT}}^{\mathrm{H}} = \boldsymbol{Z}_{\mathrm{AT}}^*$, due to reciprocity, yields

$$P_{\mathrm{Tx}} = \mathrm{E}\left[\boldsymbol{i}_{\mathrm{A}}^{\mathrm{H}}\mathrm{Re}\{\boldsymbol{Z}_{\mathrm{AT}}\}\boldsymbol{i}_{\mathrm{A}}\right]. \tag{41}$$

Assuming lossless antennas, $P_{\mathrm{Tx}} = P_{\mathrm{rad}}$ must hold true. The real part of the impedance matrix $\boldsymbol{Z}_{\mathrm{AT}}$ can therefore readily be obtained from equating (41) with (40).

C. Uniform Linear Array of Isotropic Antennas

If the antennas of the array are isotropic, then $|\alpha(\theta,\phi)|^2$ does *not* depend on θ and ϕ and hence is a constant

$$|\alpha(\theta,\phi)|^2 = \alpha_0^2 = \mathrm{const}. \tag{42}$$

By using this expression in (40) and equating the result with (41), we can express the real part of $\boldsymbol{Z}_{\mathrm{AT}}$ as

$$\mathrm{Re}\{\boldsymbol{Z}_{\mathrm{AT}}\} = R_{\mathrm{r}}\cdot\boldsymbol{C}_{\mathrm{T}} \tag{43}$$

where $R_{\mathrm{r}} = 4\pi\alpha_0^2/Z_0 > 0$ is the *radiation resistance* and

$$\boldsymbol{C}_{\mathrm{T}} = \frac{1}{2}\int_0^{\pi}\boldsymbol{a}^*(\theta)\boldsymbol{a}^{\mathrm{T}}(\theta)\sin\theta\mathrm{d}\theta \tag{44}$$

is a dimensionless matrix with the property

$$(\boldsymbol{C}_{\mathrm{T}})_{i,i} = 1 \qquad \forall i. \tag{45}$$

Because $\boldsymbol{C}_{\mathrm{T}}$ depends on the mutual distances between the antennas and the latter depend on the spatial arrangement of the antennas, we consider a simple arrangement: the *uniform linear array*, where the antennas are aligned along the (negative) z-axis. To this end, we generalize the array steering vector from (38) to the case of N antennas

$$\boldsymbol{a}(\theta)=\left[1\ \mathrm{e}^{-\mathrm{j}kd\cos\theta}\ \mathrm{e}^{-2\mathrm{j}kd\cos\theta}\ \cdots\ \mathrm{e}^{-(N-1)\mathrm{j}kd\cos\theta}\right]^{\mathrm{T}} \quad (46)$$

where d is the distance between neighboring antennas. When we apply (46) in (44) and integrate, we arrive at

$$\boldsymbol{C}_{\mathrm{T}}=\boldsymbol{C}_N \quad (47)$$

where

$$\boldsymbol{C}_K=\begin{bmatrix} 1 & j_0(kd) & j_0(2kd) & j_0(3kd) & \cdots \\ j_0(kd) & 1 & j_0(kd) & j_0(2kd) & \ddots \\ \vdots & \ddots & \ddots & \ddots & \ddots \end{bmatrix}\in\mathbb{R}^{K\times K} \quad (48)$$

$$j_0(x)=\frac{\sin x}{x} \quad (49)$$

while the index K specifies the dimension of the matrix. Note that $\boldsymbol{C}_K$ is a real-valued Toeplitz matrix which happens to be positive definite for $d>0$. The last property follows from the fact that the radiated power is always nonnegative, regardless of what excitation currents are used, and $R_{\mathrm{r}}>0$. Because (49) has zeros for $kd\in\pi\cdot\mathbb{N}$, we see that (since $k=2\pi/\lambda$)

$$\frac{2d}{\lambda}\in\mathbb{N}\iff\boldsymbol{C}_K=\mathbf{I}_K. \quad (50)$$

When we align isotropic antennas in such a way that all mutual distances are integer multiples of half the wavelength, the mutual coupling completely disappears. On the other hand, as $d\to 0$, the matrix $\boldsymbol{C}_K$ tends to the all-one matrix, such that its smallest eigenvalue $\xi\to 0$. Recalling the discussion of the unilateral approximation from Section II-F, we therefore see with the help of (15) that the critical distance between the transmitter and the receiver increases unboundedly as $d\to 0$. Hence, the antenna separation cannot be made arbitrarily small without having to move the receiver arbitrarily far away from the transmitter. However, we will see that most of the effects of mutual coupling on the performance of the communication system already occur for rather moderate values of d.

Regarding the receive impedance matrix $\boldsymbol{Z}_{\mathrm{AR}}$, we have

$$\mathrm{Re}\{\boldsymbol{Z}_{\mathrm{AR}}\}=R_{\mathrm{r}}\cdot\boldsymbol{C}_{\mathrm{R}}=R_{\mathrm{r}}\cdot\boldsymbol{C}_M. \quad (51)$$

D. Transimpedance Matrix

Finding the mutual coupling between the antennas of the receiver and the transmitter is complicated by the fact that the mutual coupling depends on the medium that connects the receiver and the transmitter. In order to keep things simple, we consider only the case where the receiver and the transmitter are located in free space. Suppose the receiver is located at elevation θ_{T} from the transmitter's point of view. Similarly, the transmitter is located at elevation θ_{R} from the receiver's point of view (see Fig. 4). Let us call $r_{m,n}$ the distance between the mth receive and nth transmit antennas. Then, $r_{m,n}=r+\Delta r_{m,n}$, where

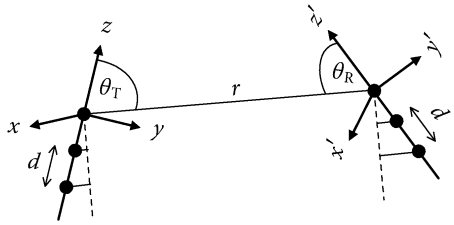

Fig. 4. Two arbitrarily oriented uniform linear arrays in free space.

$$\Delta r_{m,n}=d(n-1)\cos(\theta_{\mathrm{T}})+d(m-1)\cos(\theta_{\mathrm{R}}) \quad (52)$$

while r is the distance between the first antenna of the transmitter and the first antenna of the receiver. The electric field vector $\vec{\boldsymbol{E}}_{m,n}$ at the mth antenna of the receiver excited by the nth antenna of the transmitter becomes

$$\vec{\boldsymbol{E}}_{m,n}=\alpha_0\frac{\mathrm{e}^{-\mathrm{j}kr}}{r}\vec{\mathbf{e}}_0\cdot\mathrm{e}^{-\mathrm{j}k\Delta r_{m,n}}\cdot i_{\mathrm{A},n}. \quad (53)$$

Recall from the discussion in Section II-D that (53) requires $\boldsymbol{i}_{\mathrm{B}}=\mathbf{0}$ such that the antennas at the receiver do not disturb the field. Herein, $\boldsymbol{i}_{\mathrm{B}}$ is the vector of the complex current envelopes of the receiver-side ports of the multi-antenna multiport (see Fig. 2). The corresponding open-circuit voltage $\boldsymbol{v}_{\mathrm{B}}$ is proportional to the strength of the total electric field

$$v_{\mathrm{B},m}=\mathrm{const}\cdot\vec{\mathbf{e}}_0\cdot\sum_{n=1}^{N}\vec{\boldsymbol{E}}_{m,n}=\gamma\sum_{n=1}^{N}\mathrm{e}^{-\mathrm{j}k\Delta r_{m,n}}\cdot i_{\mathrm{A},n}\qquad\forall m \quad (54)$$

where $\gamma\in\mathbb{C}\cdot\Omega$ is a constant and $\boldsymbol{i}_{\mathrm{B}}=\mathbf{0}$. With the transmit and receive array steering vectors

$$\boldsymbol{a}_{\mathrm{T}}(\theta)=\left[1\mathrm{e}^{-\mathrm{j}kd\cos\theta}\mathrm{e}^{-2\mathrm{j}kd\cos\theta}\cdots\mathrm{e}^{-(N-1)\mathrm{j}kd\cos\theta}\right]^{\mathrm{T}} \quad (55)$$

$$\boldsymbol{a}_{\mathrm{R}}(\theta)=\left[1\mathrm{e}^{-\mathrm{j}kd\cos\theta}\mathrm{e}^{-2\mathrm{j}kd\cos\theta}\cdots\mathrm{e}^{-(M-1)\mathrm{j}kd\cos\theta}\right]^{\mathrm{T}} \quad (55a)$$

we can write (54) as

$$\boldsymbol{v}_{\mathrm{B}}=\gamma\boldsymbol{a}_{\mathrm{R}}(\theta_{\mathrm{R}})\boldsymbol{a}_{\mathrm{T}}^{\mathrm{T}}(\theta_{\mathrm{T}})\boldsymbol{i}_{\mathrm{A}},\qquad\boldsymbol{i}_{\mathrm{B}}=\mathbf{0}. \quad (56)$$

Comparison with (13) then reveals that

$$\boldsymbol{Z}_{\mathrm{ART}}=\gamma\boldsymbol{a}_{\mathrm{R}}(\theta_{\mathrm{R}})\boldsymbol{a}_{\mathrm{T}}^{\mathrm{T}}(\theta_{\mathrm{T}}). \quad (57)$$

IV. Array Gain

A proper choice of the generator voltage envelopes makes the electromagnetic fields which are excited by the transmit-side antennas superimpose coherently in a given direction, hence producing there a peak in the power density. Similarly, the superposition of the receive voltage envelopes with suitably chosen combining coefficients makes the receiver more sensitive for waves impinging from certain directions. Both effects can be

used for communications for the increase of SNR at the receiver. This increase is quantified by the so-called *array gain*

$$A \stackrel{\mathbf{def}}{=} \left.\frac{\max \mathrm{SNR}}{\mathrm{SNR}|_{M=N=1}}\right|_{P_{\mathrm{Tx}}=\mathrm{const}}. \tag{58}$$

Hence, the largest SNR, obtainable by using all antennas simultaneously is compared with the SNR, obtainable when only one transmit ($N = 1$) and one receive antenna ($M = 1$) are used, while the same transmit power P_{Tx} is employed in both cases.

Let $\boldsymbol{v}_{\mathrm{G}} = \boldsymbol{t}v_{\mathrm{G}}$, where $\boldsymbol{t} \in \mathbb{C}^{N\times 1}$ is called *transmit beamforming vector* and $v_{\mathrm{G}} \in \mathbb{C}\cdot V$ is the information-carrying signal to be transferred to the receiver. Let $v_{\mathrm{L}} = \boldsymbol{r}^{\mathrm{H}}\boldsymbol{v}_{\mathrm{L}}$ be the superposition of all receive voltage envelopes, where $\boldsymbol{r} \in \mathbb{C}^{M\times 1}$ is called *receive beamforming vector*. With (16), (23), and (25), we have

$$\mathrm{SNR} = 4P_{\mathrm{Tx}} \cdot \frac{|\boldsymbol{r}^{\mathrm{H}}\boldsymbol{D}\boldsymbol{t}|^2}{(\boldsymbol{t}^{\mathrm{H}}\boldsymbol{B}\boldsymbol{t})(\boldsymbol{r}^{\mathrm{H}}\boldsymbol{R}_{\boldsymbol{\eta}}\boldsymbol{r})}. \tag{59}$$

The maximization in (58) is therefore to be understood as an unconstrained maximization with respect to $\boldsymbol{t}$ and $\boldsymbol{r}$. It makes sense to distinguish between the *transmit array gain*

$$A_{\mathrm{Tx}} = A|_{M=1} \tag{60}$$

and the *receive array gain*

$$A_{\mathrm{Rx}} = A|_{N=1} \tag{61}$$

because both are not necessarily the same despite the fact that all multiports are reciprocal.

A. Transmit Array Gain

We have $M = 1$ receive antenna, such that $\boldsymbol{D} = \boldsymbol{d}^{\mathrm{T}} \in \mathbb{C}^{1\times N}$ is a row vector, and the SNR from (59) becomes

$$\mathrm{SNR} = \frac{4P_{\mathrm{Tx}}}{R_\eta} \cdot \frac{|\boldsymbol{d}^{\mathrm{T}}\boldsymbol{t}|^2}{\boldsymbol{t}^{\mathrm{H}}\boldsymbol{B}\boldsymbol{t}}. \tag{62}$$

The SNR is largest [31] for

$$\boldsymbol{t} = \kappa\boldsymbol{B}^{-1}\boldsymbol{d}^* = \boldsymbol{v}_{\mathrm{G}}/v_{\mathrm{G}} \tag{63}$$

where $\kappa \neq 0$ is an arbitrary constant such that the maximum SNR becomes

$$\max \mathrm{SNR} = \frac{4P_{\mathrm{Tx}}}{R_\eta} \cdot \boldsymbol{d}^{\mathrm{T}}\boldsymbol{B}^{-1}\boldsymbol{d}^*. \tag{64}$$

With (58), it then follows that

$$A_{\mathrm{Tx}} = \frac{\boldsymbol{d}^{\mathrm{T}}\boldsymbol{B}^{-1}\boldsymbol{d}^*}{(\boldsymbol{d}^{\mathrm{T}}\boldsymbol{B}^{-1}\boldsymbol{d}^*)|_{N=1}}. \tag{65}$$

From (17), (24), (57), and the third line of (19), it follows that

$$\boldsymbol{d}^{\mathrm{T}}\boldsymbol{B}^{-1}\boldsymbol{d}^* = \zeta \cdot \boldsymbol{a}_{\mathrm{T}}^{\mathrm{T}}(\theta_{\mathrm{T}}) \left(\boldsymbol{F}_{\mathrm{T}}^{-*}\mathrm{Re}\{\boldsymbol{Z}_{\mathrm{T}}\}\boldsymbol{F}_{\mathrm{T}}^{-\mathrm{T}}\right)^{-1} \boldsymbol{a}_{\mathrm{T}}^*(\theta_{\mathrm{T}}) \tag{66}$$

where $\zeta = (1/4)|Q|^2|F_{\mathrm{R}}|^2|\gamma|^2/R$, as $\boldsymbol{Q}$ and $\boldsymbol{F}_{\mathrm{R}}$ are scalars in the case $M = 1$. When we assume lossless impedance matching multiports, we have $\boldsymbol{Z}_{\mathrm{MT}}^* = -\boldsymbol{Z}_{\mathrm{MT}}$. Hence, using the second line of (19), it follows that $\mathrm{Re}\{\boldsymbol{Z}_{\mathrm{T}}\} = (1/2)(\boldsymbol{F}_{\mathrm{T}}^* - \boldsymbol{F}_{\mathrm{T}})\boldsymbol{Z}_{\mathrm{MT21}}$. Therefore

$$\boldsymbol{F}_{\mathrm{T}}^{-*}\mathrm{Re}\{\boldsymbol{Z}_{\mathrm{T}}\}\boldsymbol{F}_{\mathrm{T}}^{-\mathrm{T}} = \frac{1}{2}\left(\mathbf{I}_N - \boldsymbol{F}_{\mathrm{T}}^{-*}\boldsymbol{F}_{\mathrm{T}}\right)\boldsymbol{Z}_{\mathrm{MT21}}\boldsymbol{F}_{\mathrm{T}}^{-\mathrm{T}}. \tag{67}$$

Furthermore (using $\boldsymbol{Z}_{\mathrm{MT}}^* = -\boldsymbol{Z}_{\mathrm{MT}}$ and $\boldsymbol{Z}_{\mathrm{MT}}^{\mathrm{T}} = \boldsymbol{Z}_{\mathrm{MT}}$)

$$\boldsymbol{F}_{\mathrm{T}}^{-*}\boldsymbol{F}_{\mathrm{T}} = -(\boldsymbol{Z}_{\mathrm{MT22}} + \boldsymbol{Z}_{\mathrm{AT}})^*(\boldsymbol{Z}_{\mathrm{MT22}} + \boldsymbol{Z}_{\mathrm{AT}})^{-1}$$
$$\boldsymbol{Z}_{\mathrm{MT21}}\boldsymbol{F}_{\mathrm{T}}^{-\mathrm{T}} = \boldsymbol{Z}_{\mathrm{MT22}} + \boldsymbol{Z}_{\mathrm{AT}}$$

such that (67) can be simplified to

$$\boldsymbol{F}_{\mathrm{T}}^{-*}\mathrm{Re}\{\boldsymbol{Z}_{\mathrm{T}}\}\boldsymbol{F}_{\mathrm{T}}^{-\mathrm{T}} = \mathrm{Re}\{\boldsymbol{Z}_{\mathrm{MT22}} + \boldsymbol{Z}_{\mathrm{AT}}\} = \mathrm{Re}\{\boldsymbol{Z}_{\mathrm{AT}}\} \tag{68}$$

where the last equality is again due to $\boldsymbol{Z}_{\mathrm{MT22}}^* = -\boldsymbol{Z}_{\mathrm{MT22}}$. When we substitute (68) into (66), we arrive at

$$\boldsymbol{d}^{\mathrm{T}}\boldsymbol{B}^{-1}\boldsymbol{d}^* = \zeta \cdot \boldsymbol{a}_{\mathrm{T}}^{\mathrm{T}}(\theta_{\mathrm{T}})\mathrm{Re}\{\boldsymbol{Z}_{\mathrm{AT}}\}^{-1}\boldsymbol{a}_{\mathrm{T}}^*(\theta_{\mathrm{T}}). \tag{69}$$

Now, setting $N = 1$ in (69) leads to

$$(\boldsymbol{d}^{\mathrm{T}}\boldsymbol{B}^{-1}\boldsymbol{d}^*)|_{N=1} = \frac{\zeta}{R_{\mathrm{r}}} \tag{70}$$

where R_{r} is the radiation resistance (note that $\boldsymbol{a}_{\mathrm{T}}(\theta_{\mathrm{T}}) = 1$ and $\mathrm{Re}\{\boldsymbol{Z}_{\mathrm{AT}}\} = R_{\mathrm{r}}$ for $N = 1$). Substituting (69) and (70) into (65) and applying (43) yields

$$A_{\mathrm{Tx}} = \boldsymbol{a}_{\mathrm{T}}^{\mathrm{T}}(\theta_T)\boldsymbol{C}_{\mathrm{T}}^{-1}\boldsymbol{a}_{\mathrm{T}}^*(\theta_{\mathrm{T}}). \tag{71}$$

Because $A_{\mathrm{Tx}} = A_{\mathrm{Tx}}^*$ and $\boldsymbol{a}_{\mathrm{T}}^{\mathrm{H}}\boldsymbol{a}_{\mathrm{T}} = N$, we can rewrite (71) in the following way:

$$A_{\mathrm{Tx}} = N \cdot \frac{\boldsymbol{a}_{\mathrm{T}}^{\mathrm{H}}(\theta_{\mathrm{T}})\boldsymbol{C}_{\mathrm{T}}^{-1}\boldsymbol{a}_{\mathrm{T}}(\theta_{\mathrm{T}})}{\boldsymbol{a}_{\mathrm{T}}^{\mathrm{H}}(\theta_{\mathrm{T}})\boldsymbol{a}_{\mathrm{T}}(\theta_{\mathrm{T}})}. \tag{72}$$

Note that the transmit array gain is *independent* of what sort of impedance matching network is used and solely depends on the following parameters:

1) number of antennas (obviously);
2) usually on the direction of beamforming θ_{T};
3) antenna separation d/λ, via $\boldsymbol{C}_{\mathrm{T}}$ and $\boldsymbol{a}_{\mathrm{T}}(\theta_{\mathrm{T}})$.

Notice that the transmit array gain is *independent* of the imaginary part of $\boldsymbol{Z}_{\mathrm{AT}}$. All that matters is its normalized real part $\boldsymbol{C}_{\mathrm{T}}$ for which we already have derived a formula for the case of isotropic radiators [see (47) and (48)].

Let us now look at the transmit array gain in several situations. First, let $d = \lambda/2$ or any integer multiple thereof. Then, from (50) and (72), it follows that

$$\frac{2d}{\lambda} \in \mathbb{N} \quad \Longrightarrow \quad A_{\mathrm{Tx}} = N. \tag{73}$$

Hence, the transmit array gain equals the number of antennas at the transmitter and is independent of the beamforming direction θ_{T}. For other values of d, however, the array gain does depend on the direction of beamforming. Let us consider two distinct directions: The first is the "end-fire" direction and points along the array axis ($\theta_{\mathrm{T}} = 0$). The other one is perpendicular to the array axis ($\theta_{\mathrm{T}} = \pi/2$) and is called "front-fire" direction.

Fig. 5 shows the transmit array gain for beamforming in the end-fire direction as a function of antenna separation d. In the

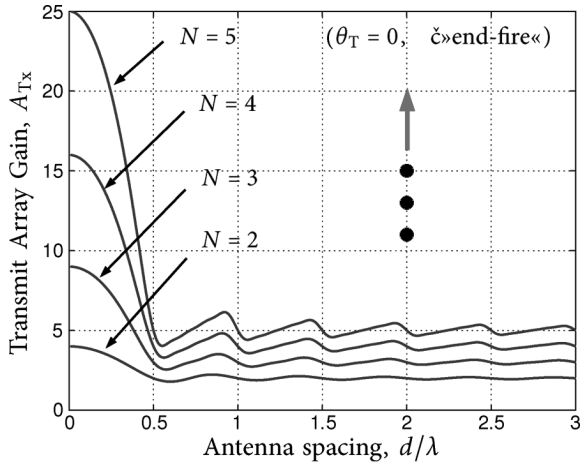

Fig. 5. Transmit array gain A_{Tx} in the end-fire direction as a function of the antenna separation for a different number N of antennas.

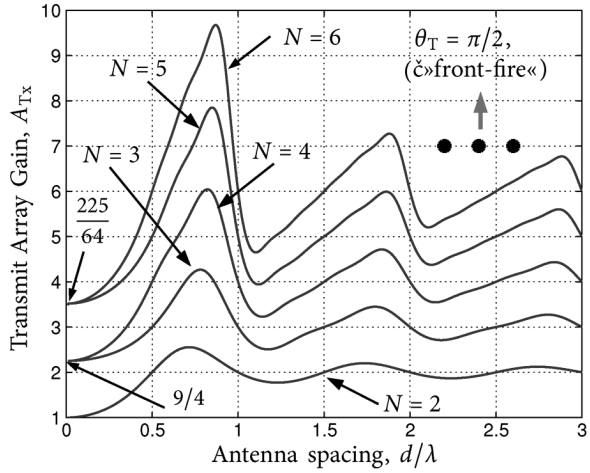

Fig. 6. Transmit array gain A_{Tx} in the front-fire direction as a function of the antenna separation for a different number N of antennas.

case when $d \gg \lambda/2$, the transmit array gain more or less equals the number N of antennas, only to raise sharply once d is reduced below $\lambda/2$. It approaches N^2 from below as $d \to 0$. However, recall from Section II-F that one cannot allow for an arbitrarily small d, for this would cause the critical distance D_{crit} between the receiver and the transmitter increase unboundedly. One can show that the smallest eigenvalue ξ of the matrix $\boldsymbol{C}_{\mathrm{T}}$ has the property $\xi = \mathrm{func}(N) \cdot (d/\lambda)^{2(N-1)} + O(d/\lambda)^{2N}$. Imagine that we have $N = 3$ closely spaced $(d \ll \lambda)$ antennas and that we decrease the antenna spacing to half. Then, ξ reduces by a factor of 16, causing the critical distance (15) to become four times as long. By allowing $N = 10$ antennas, this increase of the critical distance would already become 512 fold. This clearly indicates that, with more antennas inside the array, we should be more conservative with a small antenna separation. On the other hand, we see from Fig. 5 that decreasing d below some limit does not increase the transmit array gain by any significant amount. In fact, a moderate separation of $\lambda/4$ ensures that the transmit array gain comes about 1 dB close to N^2. In particular, for a moderate number of antennas, those large array gains can indeed be realized, as is confirmed by experimental results with monopole antennas [32], [33].

Fig. 6 shows the transmit array gain in the front-fire direction. For efficient beamforming, one has to put the antennas considerably apart. As can be seen, there is a finite optimum antenna separation which is always larger than $\lambda/2$ but smaller than λ. In the front-fire direction, the transmit array gain grows linearly with the number of antennas, yet its maximum value is larger than N. It is intriguing that as $d \to 0$, there is no difference between $2N - 1$ and $2N$ antennas with respect to transmit array gain.

Another interesting problem arises when the number of antennas is increased while the length L of the uniform linear antenna array is kept constant such that

$$d = \frac{L}{N-1}.$$

The array becomes more and more densely packed as we increase the number of antennas. How much transmit array gain is obtainable in this case? Fig. 7 shows the result for beamforming

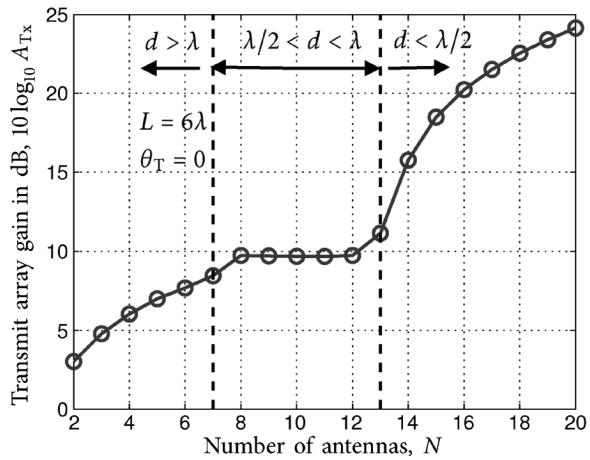

Fig. 7. Transmit array gain in decibels (!) for a fixed array size and beamforming in the end-fire direction.

in the end-fire direction and $L = 6\lambda$. Note that the transmit array gain is given in decibels. For a small N, the antenna separation is large $(d > \lambda)$ such that mutual antenna coupling is relatively low and the transmit array gain behaves more or less like that when no coupling was present. However, once N is large enough such that the distance reduces somewhat below λ, the transmit array gain essentially stays constant (actually, it drops a little bit). The reason for this peculiar behavior can be found in Fig. 5: When d is within the range aforementioned, the transmit array gain reduces with decreasing distance in a way which compensates the increase which comes from having larger N values. This continues until N is large enough such that the antenna separation drops below $\lambda/2$. Then, the transmit array approaches a quadratic growth with respect to N. The transmit array gain in the end-fire direction is theoretically unbounded—there is no hard limit for the transmit array gain that can be achieved by an antenna array of any fixed size.

For beamforming in the front-fire direction, the situation is rather different, as we can see from Fig. 8 which shows the transmit array gain in linear scaling. As N is increased such that d drops for the first time below λ, the transmit array gain makes a sudden jump. It roughly doubles its value when going

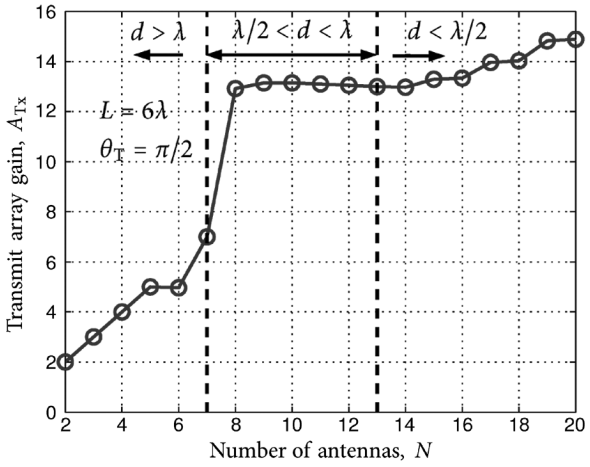

Fig. 8. Transmit array gain (*linear* scaling) for a fixed array size and beamforming in the front-fire direction.

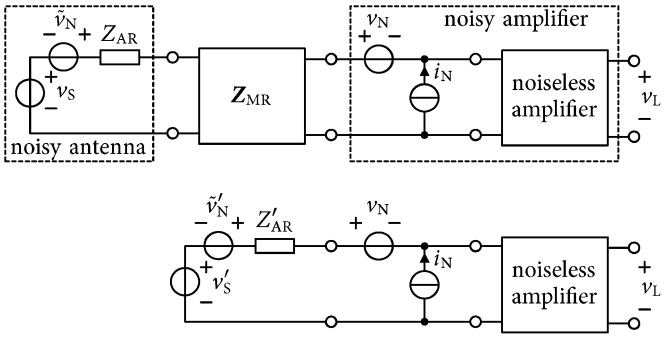

Fig. 9. (Top) Noisy single-antenna receiver. (Bottom) Equivalent circuit.

from seven to eight antennas. This effect can be understood by looking back at Fig. 6: In the front-fire direction, the maximum transmit array gain occurs for a separation d, which is slightly below λ. As a further decrease of d leads to a decreasing transmit array gain, there is once more a compensation effect, such that in Fig. 8, the transmit array gain remains almost constant (it actually drops a little bit) as N is increased. Only when N becomes large enough such that d is reduced below half the wavelength does the strong mutual coupling cause the transmit array gain to grow again, however very slowly and irregularly.

B. Noise Matching

In contrast to the transmit array gain, the receive array gain does depend on receiver impedance matching. Consequently, it makes sense to talk about the important technique of *noise matching* first, before approaching the receive array gain. Let us start with a single receive antenna. For this case, the circuit shown in the upper part of Fig. 9 is equivalent to the system shown in Fig. 2. The single receive antenna port is modeled here by its Thévenin/Helmholtz equivalent: two voltage sources with complex envelopes v_{S} and $\tilde{v}_{\mathrm{N}}$ for the signal voltage and the received noise, respectively, and a series impedance equal to the antenna impedance Z_{AR}. The job of the impedance matching twoport is to transform the antenna impedance from Z_{AR} into Z'_{AR}. Therefore, it makes sense to use the equivalent circuit shown in the lower part of Fig. 9, where the matched antenna is modeled by two voltage sources with complex envelopes v'_{S} and $\tilde{v}'_{\mathrm{N}}$, respectively, and a series impedance Z'_{AR}. Because the impedance matching network is lossless, it can be shown (see Appendix B) that

$$\mathrm{E}\left[|v'_{\mathrm{S}}|^2\right] = \mathrm{E}\left[|v_{\mathrm{S}}|^2\right] \cdot \frac{\mathrm{Re}\left\{Z'_{\mathrm{AR}}\right\}}{\mathrm{Re}\{Z_{\mathrm{AR}}\}}. \tag{74}$$

Since the same transformation has to hold for the noise voltage envelope $\tilde{v}_{\mathrm{N}}$, we have with (9) and (6)

$$\mathrm{E}\left[|\tilde{v}'_{\mathrm{N}}|^2\right] = 4\mathrm{k}T_{\mathrm{A}}\Delta f \mathrm{Re}\left\{Z'_{\mathrm{AR}}\right\}. \tag{75}$$

By letting v_{LN} be the noise part of the output voltage envelope

$$v_{\mathrm{LN}} = \eta \cdot (\tilde{v}'_{\mathrm{N}} + Z'_{\mathrm{AR}} i_{\mathrm{N}} - v_{\mathrm{N}}) \tag{76}$$

where η is a complex number (depending on the amplifier's network properties), which we do not have to worry about, however, for it will cancel out later. The signal voltage envelope at the amplifier's output equals $v_{\mathrm{LS}} = \eta \cdot v'_{\mathrm{S}}$ and with (74)

$$\mathrm{E}\left[|v_{\mathrm{LS}}|^2\right] = \frac{|\eta|^2 \mathrm{E}\left[|v_{\mathrm{S}}|^2\right]}{\mathrm{Re}\{Z_{\mathrm{AR}}\}} \cdot \mathrm{Re}\left\{Z'_{\mathrm{AR}}\right\}. \tag{77}$$

The SNR at the output can be defined as

$$\mathrm{SNR} = \frac{\mathrm{E}\left[|v_{\mathrm{LS}}|^2\right]}{\mathrm{E}\left[|v_{\mathrm{LN}}|^2\right]} = \frac{\mathrm{SNR}_{\mathrm{avail}}}{\mathrm{NF}} \tag{78}$$

where

$$\mathrm{SNR}_{\mathrm{avail}} = \frac{\mathrm{E}\left[|v_{\mathrm{S}}|^2\right] / (4\mathrm{Re}\{Z_{\mathrm{AR}}\})}{\mathrm{k}T_{\mathrm{A}}\Delta f} \tag{79}$$

is the *available* SNR, defined as the ratio of the signal power and noise power delivered into a matched load, and NF is the famous *noise figure* [34]. With (75)–(79), we find

$$\mathrm{NF} = 1 + \frac{\mathrm{E}\left[|i_{\mathrm{N}}|^2\right]}{4\mathrm{k}T_{\mathrm{A}}\Delta f} \frac{\left|Z'_{\mathrm{AR}}\right|^2}{\mathrm{Re}\left\{Z'_{\mathrm{AR}}\right\}} \cdot \left(1 - \frac{2R_{\mathrm{N}}\mathrm{Re}\left\{Z'^{*}_{\mathrm{AR}}\rho\right\}}{\left|Z'_{\mathrm{AR}}\right|^2} + \frac{R_{\mathrm{N}}^2}{\left|Z'_{\mathrm{AR}}\right|^2}\right) \tag{80}$$

wherein R_{N} and ρ are defined in (11) and (12), respectively. It is easy to show that NF is minimum for

$$Z'_{\mathrm{AR}} = Z_{\mathrm{opt}} = R_{\mathrm{N}} \cdot \left(\sqrt{1 - (\mathrm{Im}\{\rho\})^2} + j \cdot \mathrm{Im}\{\rho\}\right). \tag{81}$$

Note that $|Z_{\mathrm{opt}}| = R_{\mathrm{N}}$ and the minimum noise figure equals

$$\mathrm{NF}_{\mathrm{min}} = 1 + \frac{\mathrm{E}\left[|i_{\mathrm{N}}|^2\right]}{2\mathrm{k}T_{\mathrm{A}}\Delta f / R_{\mathrm{N}}} \cdot \left(\sqrt{1 - (\mathrm{Im}\{\rho\})^2} - \mathrm{Re}\{\rho\}\right). \tag{82}$$

The case of more than a single antenna at the receiver is complicated by mutual antenna coupling. In this case, one reduces the

problem back into the single-antenna case [35] by employing an impedance matching network which *decouples* the antennas. Hence, the receive impedance matrix of the matched antenna array becomes

$$\boldsymbol{Z}_{\mathrm{R}} = Z_{\mathrm{opt}}\mathbf{I}_M. \tag{83}$$

With the topmost equations in (19) and (20), a lossless reciprocal impedance matching network described by (84), as shown at the bottom of the page, gets the job done nicely. Note that, from (19), there is

$$\boldsymbol{Z}_{\mathrm{RT}} = \mathrm{j}\sqrt{\mathrm{Re}\{Z_{\mathrm{opt}}\}}\mathrm{Re}\{\boldsymbol{Z}_{\mathrm{AR}}\}^{-1/2}\boldsymbol{Z}_{\mathrm{ART}}\boldsymbol{F}_{\mathrm{T}}^{\mathrm{T}}. \tag{85}$$

Even though the receive-side antennas are *de*coupled, the mutual antenna coupling sneaks into the transimpedance matrix of the matched system via the matrix $\mathrm{Re}\{\boldsymbol{Z}_{\mathrm{AR}}\}$. Therefore, *a decoupled antenna array is substantially different from an array of uncoupled antennas*.

C. Receive Array Gain

We have $N = 1$ transmit antenna, such that $\boldsymbol{D} = \boldsymbol{d} \in \mathbb{C}^{M\times 1}$ is a column vector, and the SNR from (59) becomes

$$\mathrm{SNR} = \frac{4P_{\mathrm{Tx}}}{B}\cdot\frac{|\boldsymbol{r}^{\mathrm{H}}\boldsymbol{d}|^2}{\boldsymbol{r}^{\mathrm{H}}\boldsymbol{R}_{\boldsymbol{\eta}}\boldsymbol{r}}. \tag{86}$$

The SNR is largest for $\boldsymbol{r} = \kappa\mathbf{R}_{\boldsymbol{\eta}}^{-1}\boldsymbol{d}$, where $\kappa \neq 0$ is an arbitrary constant such that the maximum SNR becomes

$$\max\mathrm{SNR} = \frac{4P_{\mathrm{Tx}}}{B}\cdot\boldsymbol{d}^{\mathrm{H}}\boldsymbol{R}_{\boldsymbol{\eta}}^{-1}\boldsymbol{d}. \tag{87}$$

With (58), it then follows that

$$A_{\mathrm{Rx}} = \frac{\boldsymbol{d}^{\mathrm{H}}\boldsymbol{R}_{\boldsymbol{\eta}}^{-1}\boldsymbol{d}}{\left(\boldsymbol{d}^{\mathrm{H}}\boldsymbol{R}_{\boldsymbol{\eta}}^{-1}\boldsymbol{d}\right)\Big|_{M=1}}. \tag{88}$$

With (18), (19), (57), and (26), we find

$$\boldsymbol{d}^{\mathrm{H}}\boldsymbol{R}_{\boldsymbol{\eta}}^{-1}\boldsymbol{d} = \zeta\cdot\boldsymbol{a}_{\mathrm{R}}^{\mathrm{H}}\boldsymbol{F}_{\mathrm{R}}^{\mathrm{H}}\boldsymbol{\Upsilon}^{-1}\boldsymbol{F}_{\mathrm{R}}\boldsymbol{a}_{\mathrm{R}} \tag{89}$$

where $\zeta = R|\gamma F_{\mathrm{T}}(R+Z_{\mathrm{T}})^{-1}|^2/(\beta R_{\mathrm{r}}^2)$, and we use $\boldsymbol{a}_{\mathrm{R}}$ as a shorthand for $\boldsymbol{a}_{\mathrm{R}}(\theta_{\mathrm{R}})$. Now, we apply the technique of noise matching. Using the impedance matching network described by (84), it can be shown (see Appendix C) that

$$\boldsymbol{\Upsilon} = \chi\cdot\sqrt{1-(\mathrm{Im}\{\rho\})^2}\left((\mathrm{NF}_{\min}-1)\mathbf{I}_M + \boldsymbol{C}_{\mathrm{R}}^{-1/2}\boldsymbol{\phi}\boldsymbol{C}_{\mathrm{R}}^{-1/2}\right) \tag{90}$$

where $\chi = (4\mathrm{k}T_{\mathrm{A}}\Delta f R_{\mathrm{N}})/(\beta R_{\mathrm{r}}^2)$. From (84) and the first line of (20), it follows that, with the help of (83) and (51)

$$\boldsymbol{F}_{\mathrm{R}} = \mathrm{j}\sqrt{\frac{R_{\mathrm{N}}}{R_{\mathrm{r}}}}\sqrt{1-(\mathrm{Im}\{\rho\})^2}\,\boldsymbol{C}_{\mathrm{R}}^{-1/2}. \tag{91}$$

When we substitute (90) and (91) into (89), we obtain

$$\boldsymbol{d}^{\mathrm{H}}\boldsymbol{R}_{\boldsymbol{\eta}}^{-1}\boldsymbol{d} = \frac{\zeta R_{\mathrm{N}}}{\chi R_{\mathrm{r}}}\cdot\boldsymbol{a}_{\mathrm{R}}^{\mathrm{H}}\left((\mathrm{NF}_{\min}-1)\boldsymbol{C}_{\mathrm{R}}+\boldsymbol{\phi}\right)^{-1}\boldsymbol{a}_{\mathrm{R}}. \tag{92}$$

By setting $M = 1$, we obtain from (92)

$$\left(\boldsymbol{d}^{\mathrm{H}}\boldsymbol{R}_{\boldsymbol{\eta}}^{-1}\boldsymbol{d}\right)\Big|_{M=1} = \frac{\zeta R_{\mathrm{N}}}{\chi R_{\mathrm{r}}}\cdot\mathrm{NF}_{\min}^{-1} \tag{93}$$

for $\boldsymbol{C}_{\mathrm{R}} = 1$ and $\boldsymbol{\phi} = 1$ when $M = 1$. By substituting (92) and (93) into (88) and using the fact that $\boldsymbol{a}_{\mathrm{R}}^{\mathrm{H}}\boldsymbol{a}_{\mathrm{R}} = M$, the receive array gain finally becomes

$$A_{\mathrm{Rx}} = M\cdot\frac{\boldsymbol{a}_{\mathrm{R}}^{\mathrm{H}}(\theta_{\mathrm{R}})\left((\mathrm{NF}_{\min}-1)\boldsymbol{C}_{\mathrm{R}}+\boldsymbol{\phi}\right)^{-1}\boldsymbol{a}_{\mathrm{R}}(\theta_{\mathrm{R}})}{\boldsymbol{a}_{\mathrm{R}}^{\mathrm{H}}(\theta_{\mathrm{R}})\boldsymbol{a}_{\mathrm{R}}(\theta_{\mathrm{R}})\cdot\mathrm{NF}_{\min}^{-1}}. \tag{94}$$

A comparison of (94) and (72) reveals that transmit and receive array gains are fairly similar, but at the same time, subtly different. Most notably, the receive array gain depends on the minimum noise figure—something for which there is no counterpart in the transmit array gain. Thus, *transmit and receive array gains are, in general, different despite the fact that all involved multiports are reciprocal*.

Notice that the minimum noise figure depends on antenna noise temperature. From (82), $\mathrm{NF}_{\min}$ at antenna noise temperature $T_{\mathrm{A},2}$ depends on $\mathrm{NF}_{\min}$ at another antenna noise temperature $T_{\mathrm{A},1}$ like $\mathrm{NF}_{\min}|_{T_{\mathrm{A}}=T_{\mathrm{A},2}} = 1 + (\mathrm{NF}_{\min}|_{T_{\mathrm{A}}=T_{\mathrm{A},1}} - 1)T_{\mathrm{A},1}/T_{\mathrm{A},2}$. If $\mathrm{NF}_{\min}$ equals, for example, 2 dB at an antenna noise temperature of 300 K, $\mathrm{NF}_{\min}$ increases to 7.3 dB, as antenna noise temperature decreases to 40 K. Similarly, $\mathrm{NF}_{\min}$ drops to 0.15 dB, when the antenna noise temperature hits 5000 K. Ultimately, as $T_{\mathrm{A}} \to \infty$, we see that $\mathrm{NF}_{\min} \to 1$ and $T_{\mathrm{A}} \to 0$ cause $\mathrm{NF}_{\min} \to \infty$. Based on this observation, we can separate three interesting cases.

1) *Noiseless antennas* ($\mathrm{NF}_{\min} \to \infty$).
   It is not possible to have noiseless antennas, yet such a situation occurs approximately in the case where the receive amplifiers are the dominating contributors to the noise. From (94), one obtains in this case

$$\lim_{\mathrm{NF}\to\infty} A_{\mathrm{Rx}} = M\cdot\frac{\boldsymbol{a}_{\mathrm{R}}^{\mathrm{H}}(\theta_{\mathrm{R}})\boldsymbol{C}_{\mathrm{R}}^{-1}\boldsymbol{a}_{\mathrm{R}}(\theta_{\mathrm{R}})}{\boldsymbol{a}_{\mathrm{R}}^{\mathrm{H}}(\theta_{\mathrm{R}})\boldsymbol{a}_{\mathrm{R}}(\theta_{\mathrm{R}})}. \tag{95}$$

$$\boldsymbol{Z}_{\mathrm{MR}} = \begin{bmatrix} \mathrm{j}\mathrm{Im}\{Z_{\mathrm{opt}}\}\mathbf{I}_M & \mathrm{j}\sqrt{\mathrm{Re}\{Z_{\mathrm{opt}}\}}\mathrm{Re}\{\boldsymbol{Z}_{\mathrm{AR}}\}^{1/2} \\ \mathrm{j}\sqrt{\mathrm{Re}\{Z_{\mathrm{opt}}\}}\mathrm{Re}\{\boldsymbol{Z}_{\mathrm{AR}}\}^{1/2} & -\mathrm{j}\mathrm{Im}\{\boldsymbol{Z}_{\mathrm{AR}}\} \end{bmatrix} \tag{84}$$

That means, for zero background noise, the receive array gain is exactly the same as the transmit array gain of the same array.

2) *Effectively noiseless amplifiers* ($\mathrm{NF}_{\min} = 1$).
This case is allowed in theory and corresponds to the situation where amplifier noise originates solely from the thermal agitation of the electrons in the real part of its input admittance. In this case, the noise resistance $R_{\mathrm{N}} = 0$, and from (82), indeed, $\mathrm{NF}_{\min} = 1$. This time

$$\lim_{\mathrm{NF}\to 1} A_{\mathrm{Rx}} = M \cdot \frac{\boldsymbol{a}_{\mathrm{R}}^{\mathrm{H}}(\theta_{\mathrm{R}})\boldsymbol{\phi}^{-1}\boldsymbol{a}_{\mathrm{R}}(\theta_{\mathrm{R}})}{\boldsymbol{a}_{\mathrm{R}}^{\mathrm{H}}(\theta_{\mathrm{R}})\boldsymbol{a}_{\mathrm{R}}(\theta_{\mathrm{R}})}. \tag{96}$$

When the antennas are the dominant noise source, then the receive array gain is usually different from the transmit array gain.

3) *Isotropic extrinsic noise* ($\boldsymbol{\phi} = \boldsymbol{C}_{\mathrm{R}}$).
In the case that the background noise which is received by the antenna array happens to have a very special covariance matrix, namely, $\boldsymbol{\phi} = \boldsymbol{C}_{\mathrm{R}}$, we find

$$\lim_{\boldsymbol{\phi}\to\boldsymbol{C}_{\mathrm{R}}} A_{\mathrm{Rx}} = M \cdot \frac{\boldsymbol{a}_{\mathrm{R}}^{\mathrm{H}}(\theta_{\mathrm{R}})\boldsymbol{C}_{\mathrm{R}}^{-1}\boldsymbol{a}_{\mathrm{R}}(\theta_{\mathrm{R}})}{\boldsymbol{a}_{\mathrm{R}}^{\mathrm{H}}(\theta_{\mathrm{R}})\boldsymbol{a}_{\mathrm{R}}(\theta_{\mathrm{R}})}. \tag{97}$$

For $\boldsymbol{\phi} = \boldsymbol{C}_{\mathrm{R}}$, the receive array gain is again equal to the transmit array gain, *regardless* of the noise figure. It can be shown (see Appendix D) that the case $\boldsymbol{\phi} = \boldsymbol{C}_{\mathrm{R}}$ is indeed possible and corresponds to *isotropic* background radiation.

D. On Scaling Laws

We have seen that transmit and receive array gains are both capable of growing as the square of the number of antennas, provided that optimum beamforming is applied in the end-fire direction. While the transmit array gain does not depend on the type of transmit impedance matching, the achievable SNR does depend on receive impedance matching. Its largest value is achieved when *noise matching* is employed. However, what happens to the SNR if a different impedance matching technique is used? It shall not come as a surprise to see that the SNR is lower than that in the case of noise matching, but how about the dependence on the number of antennas?

To this end, let us introduce a different matching technique and refer to it as *IZ-matching*. Herein, the receive impedance matching multiport is described by

$$\boldsymbol{Z}_{\mathrm{MR}} = \mathrm{j}\begin{bmatrix} \mathbf{O}_M & \mathrm{Re}\{\boldsymbol{Z}_{\mathrm{AR}}\} \\ \mathrm{Re}\{\boldsymbol{Z}_{\mathrm{AR}}\} & -\mathrm{Im}\{\boldsymbol{Z}_{\mathrm{AR}}\} \end{bmatrix}.$$

As can be easily verified from the first line of (19), this causes $\boldsymbol{Z}_{\mathrm{R}} = \mathrm{Re}\{\boldsymbol{Z}_{\mathrm{AR}}\}$. Hence, the effect of this matching technique is to remove the imaginary part of $\boldsymbol{Z}_{\mathrm{AR}}$ and keep its real part as is. The antennas therefore remain coupled. Let us now see what maximum SNR can be achieved using IZ-matching and compare it to the case of noise matching. One merely has to evaluate (87) separately for those two matching techniques.

There is a single transmit antenna positioned in the end-fire direction of the receiver ($\theta_{\mathrm{R}} = 0$). We set the noise parameters as $\tilde{\beta}/\beta = R_{\mathrm{N}}/R_{\mathrm{r}} = 10^{-3}$, $\rho = 0$, and $\boldsymbol{\phi} = \boldsymbol{C}_{\mathrm{R}}$. The distance between the neighboring antennas of the receive array is $d = \lambda/4$. Fig. 10 shows the resulting maximum SNR

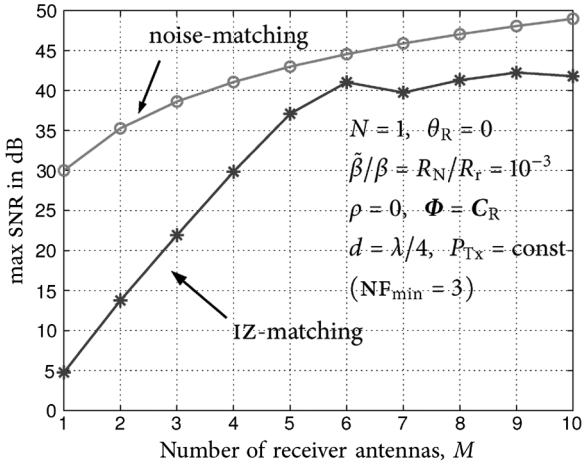

Fig. 10. Maximum SNR as a function of antenna number at the receiver for different matching techniques and constant transmit power.

in decibels as a function of the number of antennas, while the transmit power is kept constant. For noise matching, we can observe an (almost) quadratic growth (6 dB per doubling the antenna number) of SNR with the antenna number. As expected, the SNR is always larger than that with IZ-matching. However, it might be surprising that, with IZ-matching, the SNR can increase *exponentially* with the antenna number. In this example, the increase is about 8 dB for each additional antenna. At a high SNR, the channel capacity is proportional to the logarithm of SNR [36] such that an exponential growth of SNR translates into a *linear* growth of channel capacity with the number of receive antennas. The linear growth of capacity is commonly—yet wrongly—attributed only to systems with multiple antennas at *both* ends of the link [2]. Of course, IZ-matching is not really favorable because it starts out with a penalty in SNR due to the impedance mismatch (in this example, about 25 dB). This penalty is never quite made up, even by exponential growth of SNR, for the latter eventually flattens out. It is an interesting phenomenon that, with IZ-matching, the SNR is not monotonic in the antenna number. In this example, going from six to seven antennas actually decreases the SNR.

V. MIMO Communications

Let us now proceed further and consider radio communication systems which employ multiple antennas at *both* ends of the system. These so-called MIMO systems have been extensively analyzed in the information theory literature, particularly for Gaussian-distributed signals and noise (e.g., [2], [27], and [37]–[39]). The MIMO system is modeled

$$\boldsymbol{y} = \boldsymbol{H}\boldsymbol{x} + \boldsymbol{\vartheta} \tag{98}$$

$$\mathrm{E}\left[\|\boldsymbol{x}\|_2^2\right] = P_{\mathrm{Tx}} \tag{98a}$$

$$\mathrm{E}[\boldsymbol{\vartheta}\boldsymbol{\vartheta}^{\mathrm{H}}] = \sigma^2\mathbf{I}_M \tag{98b}$$

where the N-dimensional vector $\boldsymbol{x}$ is called "channel input," the M-dimensional vector $\boldsymbol{y}$ is called the "channel output," while $\boldsymbol{\vartheta}$ is the vector of zero-mean, additive, white, complex, and circularly symmetric Gaussian noise. The matrix $\boldsymbol{H} \in \mathbb{C}^{M\times N}$ is called the channel matrix. For a given channel matrix, the channel capacity of the MIMO system can be computed [2].

It is part of the beauty of information theory that one *does not have to*—and usually does not—define what the channel input and output actually are, i.e., how they are related with measurable quantities (physical quantities) of the communication system. By this abstract approach, (98)–(98b) can be used to model a great variety of communication systems.

In order to successfully apply information theory to a particular communication system—successful in the sense that the predictions of the theory can stand the test of actual measurement—one has to encode the *physical context* of the system into the channel matrix. It must make a difference in the way we build the channel matrix, when, at one time, our MIMO system is a multiwire on-chip bus and, another time, a multi-antenna radio communication system, for the governing physics is different for the two. However, how does one encode the physical context into the channel matrix?

A. Channel Matrix

We find the channel matrix when we define the relationships between $\boldsymbol{x}$ and $\boldsymbol{y}$ on the one hand and the physical quantities of the communication system on the other. Because of (98a), whatever that relationship may be, $\mathrm{E}[\|\boldsymbol{x}\|_2^2]$ has to equal the (physical) transmit power of the communication system. Using our circuit theoretic system model from Section II, it makes sense to associate the channel input $\boldsymbol{x}$ with the vector of the complex generator voltage envelopes $\boldsymbol{v}_\mathrm{G}$. By defining

$$\boldsymbol{x} = \frac{1}{2\sqrt{R}}\boldsymbol{B}^{1/2}\boldsymbol{v}_\mathrm{G} \tag{99}$$

we make sure that (98a) holds true, as is easily verified by substituting (99) into (98a) and comparing the result with (23). Note that because $\boldsymbol{B}$ is Hermitian positive definite, $\boldsymbol{B}^{1/2}$ is also Hermitian positive definite. Similarly, by associating $\boldsymbol{y}$ with the vector $\boldsymbol{v}_\mathrm{L}$ of the complex voltage envelopes at the receiver output and defining

$$\boldsymbol{y} = \sqrt{\frac{\sigma^2}{R}}\boldsymbol{R}_{\boldsymbol{\eta}}^{-1/2}\boldsymbol{v}_\mathrm{L} \tag{100}$$

we make sure that (98b) holds true. This follows from

$$\mathrm{E}[\boldsymbol{\vartheta}\boldsymbol{\vartheta}^\mathrm{H}] = \mathrm{E}[\boldsymbol{y}\boldsymbol{y}^\mathrm{H}|\boldsymbol{x} = \boldsymbol{0}]$$

and the application of (16). Notice that $\boldsymbol{x} = \boldsymbol{0}$ means that $\boldsymbol{v}_\mathrm{G} = \boldsymbol{0}$ and vice versa, for $\boldsymbol{B}$ is positive definite and hence regular. We are now almost set, but we still need one more assumption: The physical noise sources of the communication system must produce a *Gaussian* noise. This is necessary because only the Gaussian distribution remains Gaussian under arbitrary linear transformations [40]. In this way, the noise part of (100) is guaranteed to be Gaussian, too. When we substitute (99) and (100) into (98) and compare with (16), we find that

$$\boldsymbol{H} = \sqrt{4\sigma^2}\boldsymbol{R}_{\boldsymbol{\eta}}^{-1/2}\boldsymbol{D}\boldsymbol{B}^{-1/2}. \tag{101}$$

The channel matrix given in (101) contains the complete physical context of the communication system.

B. Matched Systems With Isotropic Background Noise

There are numerous factors, including the impedance matching and the background noise correlation, which have impact on the channel matrix. However, matters are simplified a great deal when one requires that specific impedance matching is used and that the background radiation is isotropic, i.e.,

$$\boldsymbol{\phi} = \boldsymbol{C}_\mathrm{R} \tag{102}$$

as shown in Appendix D. We have seen in Section IV-B that it does make good sense to employ *noise matching* [see (84)] at the receiver. On the other hand, recall from Section IV-A that transmit matching has no influence on the transmit array gain. One could therefore use just about any kind of transmit matching strategy. Both from a practical view point and for mathematical convenience, it makes sense to choose the *power matching* technique for the transmitter

$$\boldsymbol{Z}_\mathrm{MT} = \begin{bmatrix} \mathbf{O}_\mathrm{N} & -\mathrm{j}\sqrt{R}\mathrm{Re}\{\boldsymbol{Z}_\mathrm{AT}\}^{1/2} \\ -\mathrm{j}\sqrt{R}\mathrm{Re}\{\boldsymbol{Z}_\mathrm{AT}\}^{1/2} & -\mathrm{j}\mathrm{Im}\{\boldsymbol{Z}_\mathrm{AT}\} \end{bmatrix}. \tag{103}$$

This ensures that $\boldsymbol{Z}_\mathrm{T} = R\mathbf{I}_\mathrm{N}$ such that all the available power of the generators is delivered into the antenna array. Defining

$$\sigma^2 = 4\mathrm{k}T_\mathrm{A}\Delta f\mathrm{NF}_\mathrm{min} \tag{104}$$

we obtain from (101)—assuming (84), (102), and (103)

$$\boldsymbol{H} = \frac{\mathrm{e}^{-\mathrm{j}\varphi}}{R_\mathrm{r}}\boldsymbol{C}_\mathrm{R}^{-1/2}\boldsymbol{Z}_\mathrm{ART}\boldsymbol{C}_\mathrm{T}^{-1/2} \tag{105}$$

where $\varphi = \mathrm{angle}(R + Z_\mathrm{opt})$. *The information theoretic channel matrix as given in* (105) *contains the essential physics of a lossless multi-antenna MIMO system which uses noise matching at the receiver and power matching at the transmitter and where, in addition to amplifier noise, there is isotropic background noise being received by the antennas*. Note that Z_opt and R only contribute to a common phase term of all entries of $\boldsymbol{H}$. Hence, they have no influence on the channel capacity. If σ^2 is given, then what one really needs to know in information theory is just the triple

$$(\boldsymbol{C}_\mathrm{R},\ \boldsymbol{C}_\mathrm{T},\ \boldsymbol{Z}_\mathrm{ART}/R_\mathrm{r}). \tag{106}$$

The physics of mutual antenna coupling is fully included by virtue of the matrices $\boldsymbol{C}_\mathrm{R}$ and $\boldsymbol{C}_\mathrm{T}$. Note that these matrices also influence the Frobenius norm of $\boldsymbol{H}$.

In information theory, one frequently uses *stochastic* channel matrices. For *correlated Rayleigh fading*, which is independent between the receiver and the transmitter [41], [42], this can be achieved by modeling $\boldsymbol{Z}_\mathrm{ART}$ as [43]

$$\boldsymbol{Z}_\mathrm{ART} = \frac{1}{\sqrt{\mathrm{tr}\boldsymbol{R}_\mathrm{Tx}}}\boldsymbol{R}_\mathrm{Rx}^{1/2}\boldsymbol{G}\boldsymbol{R}_\mathrm{Tx}^{1/2} \tag{107}$$

where $\mathbf{R}_\mathrm{Tx} = \mathrm{E}[\boldsymbol{Z}_\mathrm{ART}^\mathrm{H}\boldsymbol{Z}_\mathrm{ART}]$ and $\mathbf{R}_\mathrm{Rx} = \mathrm{E}[\boldsymbol{Z}_\mathrm{ART}\boldsymbol{Z}_\mathrm{ART}^\mathrm{H}]$ are the transmit and receive fading correlation matrices, respectively, while the matrix $\boldsymbol{G} \in \mathbb{C}^{M\times N}$ contains independent

and identically distributed (i.i.d.) zero-mean and unity-variance complex Gaussian entries.

C. Channel Rank of Densely Packed Antenna Arrays

One of the key properties of MIMO systems is their ability to transfer multiple data streams at the same time using the same band of frequencies. For example, consider a system with two antennas at each end of the link. Let

$$\boldsymbol{H} = \boldsymbol{U}\begin{bmatrix} s_1 & 0 \\ 0 & s_2 \end{bmatrix}\boldsymbol{V}^{\mathrm{H}}$$

be the singular value decomposition of $\boldsymbol{H}$, where $\boldsymbol{U}, \boldsymbol{V} \in \mathbb{C}^{2\times 2}$ are unitary matrices and $s_1 \geq 0$ and $s_2 \geq 0$ are its two singular values. In new variables $\boldsymbol{x}' = \boldsymbol{V}^{\mathrm{H}}\boldsymbol{x}$ and $\boldsymbol{y}' = \boldsymbol{U}^{\mathrm{H}}\boldsymbol{y}$, we obtain from (98)

$$\boldsymbol{y}' = \begin{bmatrix} s_1 & 0 \\ 0 & s_2 \end{bmatrix}\boldsymbol{x}' + \boldsymbol{\vartheta}'$$

where $\boldsymbol{\vartheta}' = \boldsymbol{U}^{\mathrm{H}}\boldsymbol{\vartheta}$. Since $\|\boldsymbol{x}'\|_2^2 = \|\boldsymbol{x}\|_2^2$ and $\mathrm{E}[\boldsymbol{\vartheta}'\boldsymbol{\vartheta}'^{\mathrm{H}}] = \mathrm{E}[\boldsymbol{\vartheta}\boldsymbol{\vartheta}^{\mathrm{H}}]$, the "primed" MIMO system aforementioned and the original system (98) are identical from an information theory view point (as long as all the signals are Gaussian distributed). However, the primed MIMO system has a diagonal channel matrix which directly shows the possibility to transfer *two* independent data streams simultaneously, without having the streams interfere with each other. Of course, this only works as long as both s_1 and s_2 are strictly positive. That is, of course, only the case when $\boldsymbol{H}$ has a full rank.

What is going to happen to the rank of the channel matrix $\boldsymbol{H}$ if the separation d between the two antennas in the transmit and receive arrays is reduced more and more? Without considering mutual coupling, the antennas ultimately look like a single antenna—the same way the MIMO system would behave as if only one antenna was present at each end of the link. In other words, without mutual coupling, the channel matrix is rank deficient; hence, its determinant vanishes as we reduce $d \to 0$. However, what is the result when we take mutual coupling into account?

To this end, let there be *two* paths connecting the transmitter to the receiver, for example, one direct path in the line of sight and another path via some reflectors. The kth path departs the transmit array in the direction $\theta_{\mathrm{T},k}$ and arrives at the receive array from the direction $\theta_{\mathrm{R},k}$, where $k \in \{1, 2\}$. The transimpedance matrix $\boldsymbol{Z}_{\mathrm{ART}}$ is then given as a linear superposition of (57) for the two paths

$$\boldsymbol{Z}_{\mathrm{ART}} = \sum_{k=1}^{2} \gamma_k \boldsymbol{a}_{\mathrm{R}}(\theta_{\mathrm{R},k})\boldsymbol{a}_{\mathrm{T}}^{\mathrm{T}}(\theta_{\mathrm{T},k}). \tag{108}$$

Note that $\boldsymbol{Z}_{\mathrm{ART}}$ converges to a scaled all-one matrix, as $d \to 0$; hence, it becomes rank deficient. However, when we substitute (108) into (105), one can show (after some lengthy algebraic calculation) that

$$\det \lim_{d\to 0} \boldsymbol{H} = -3\zeta^2\gamma_1\gamma_2\left(\cos(\theta_{\mathrm{R},1}) - \cos(\theta_{\mathrm{R},2})\right) \times \left(\cos(\theta_{\mathrm{T},1}) - \cos(\theta_{\mathrm{T},2})\right)$$

where $\zeta = \mathrm{e}^{-\mathrm{j}\varphi}/R_{\mathrm{r}}$. *Effective multistreaming is possible irrespective of how densely the antennas are packed.* In order to demonstrate this effect in an even more striking way, let us consider

$$\begin{aligned} \theta_{\mathrm{R},1} &= \theta_{\mathrm{T},2} = \pi/2 - \arccos\sqrt{2/3} \approx 55^\circ \\ \theta_{\mathrm{R},2} &= \theta_{\mathrm{T},1} = \pi/2 + \arccos\sqrt{2/3} \approx 125^\circ \\ \gamma_1 &= \gamma_2 = \gamma. \end{aligned}$$

The channel matrix now becomes, as $d \to 0$

$$\lim_{d\to 0} \boldsymbol{H} = 2\zeta\gamma\begin{bmatrix} 1 & 0 \\ 0 & 1 \end{bmatrix}.$$

This intriguing result shows that it is possible to transfer two data streams free of mutual interference, which are even capable to carry *the same* information rate, despite the fact that $d \to 0$. Of course, d cannot really be arbitrarily small as we have pointed out in Section IV-A. However, we can anticipate that wireless MIMO systems comprising compact antenna arrays (minimum antenna spacing below half the wavelength) have the potential for multistreaming.

VI. Lossy Antennas—Array Gain and Efficiency

Up to now, only lossless antennas were considered in this paper. However, while antennas may not have too much loss, the little loss they have may become important, in case comparatively large electric currents have to flow in order to radiate a given power. In particular, for very low antenna separation, the losses inside the antenna can strongly reduce the array gain. It is therefore important to carefully design the antenna separation.

In the following, we assume ohmic losses in the transmitter-side antennas. The real part of the transmit impedance matrix then becomes

$$\mathrm{Re}\{\boldsymbol{Z}_{\mathrm{AT}}\} = R_{\mathrm{d}}\mathbf{I}_{\mathrm{N}} + R_{\mathrm{r}}\boldsymbol{C}_{\mathrm{T}} = R_{\mathrm{r}}\left(\boldsymbol{C}_{\mathrm{T}} + \frac{R_{\mathrm{d}}}{R_{\mathrm{r}}}\mathbf{I}_{\mathrm{N}}\right) \tag{109}$$

where $R_{\mathrm{d}} > 0$ is the *dissipation resistance* of each antenna.

A. Transmit Array Gain of Lossy Antenna Arrays

The transmit array gain for a lossy array is defined as

$$A_{\mathrm{Tx}} \stackrel{\mathbf{def}}{=} \left.\frac{\max \mathrm{SNR}|_{M=1}}{\mathrm{SNR}|_{\substack{M=N=1 \\ R_{\mathrm{d}}=0}}}\right|_{P_{\mathrm{Tx}}=\mathrm{const}}. \tag{110}$$

Therefore, the maximum SNR achievable by using all N *lossy* antennas at the transmitter is compared with the SNR achievable when only one single *but lossless* antenna is employed at the transmitter, while the same transmit power is used in both cases. Note that transmit power is defined as the power flowing into the antenna array. Since the antennas are lossy now, the transmit power is larger than the radiated power.

The denominator of (110) is very similar to that of (58); the only difference is that, in the numerator of (110), we have to cater for the antenna losses. With (109), we only have to replace in (72) the matrix $\boldsymbol{C}_{\mathrm{T}}$ by $(\boldsymbol{C}_{\mathrm{T}} + (R_{\mathrm{d}}/R_{\mathrm{r}})\mathbf{I}_{\mathrm{N}})$

$$A_{\mathrm{Tx}} = N \cdot \frac{\boldsymbol{a}_{\mathrm{T}}^{\mathrm{H}}(\theta_{\mathrm{T}})\left(\boldsymbol{C}_{\mathrm{T}} + \frac{R_{\mathrm{d}}}{R_{\mathrm{r}}}\mathbf{I}_{\mathrm{N}}\right)^{-1}\boldsymbol{a}_{\mathrm{T}}(\theta_{\mathrm{T}})}{\boldsymbol{a}_{\mathrm{T}}^{\mathrm{H}}(\theta_{\mathrm{T}})\boldsymbol{a}_{\mathrm{T}}(\theta_{\mathrm{T}})}. \tag{111}$$

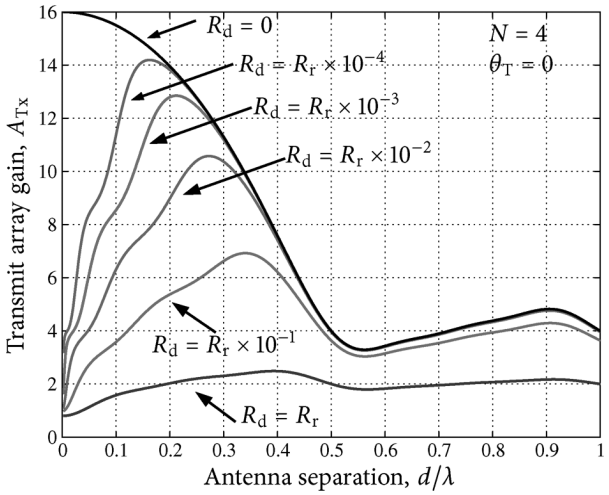

Fig. 11. Transmit array gain of a lossy array of isotrops with beamforming in the end-fire direction.

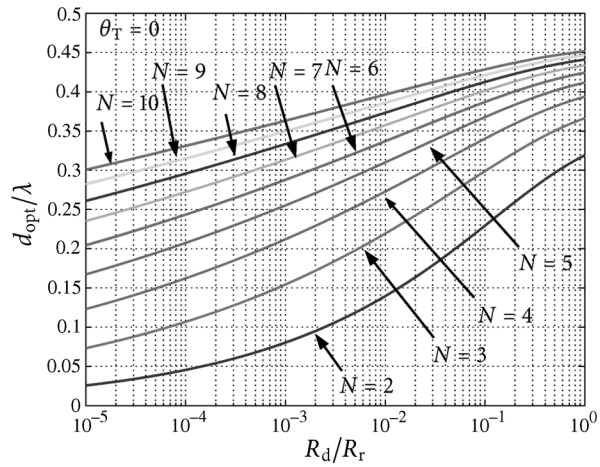

Fig. 12. Optimum antenna separation for end-fire beamforming as a function of the amount of loss $(R_{\mathrm{d}}/R_{\mathrm{r}})$.

It is easy to see that

$$A_{\mathrm{Tx}}|_{R_{\mathrm{d}}>0} < A_{\mathrm{Tx}}|_{R_{\mathrm{d}}=0} \tag{112}$$

for $\boldsymbol{C}_{\mathrm{T}}^{-1}$ and $(\boldsymbol{C}_{\mathrm{T}}+(R_{\mathrm{d}}/R_{\mathrm{r}})\mathbf{I}_N)^{-1}$ have the same eigenvectors, but the latter has smaller corresponding eigenvalues, because $\boldsymbol{C}_{\mathrm{T}}$ is positive definite and $R_{\mathrm{d}}/R_{\mathrm{r}} > 0$.

Fig. 11 shows the transmit array gain as evaluated from (111) and beamforming in the end-fire direction and a uniform linear array of $N = 4$ isotropic antennas. For lossless antennas ($R_{\mathrm{d}} = 0$), the largest array gain is achieved as $d \to 0$ and approaches N^2 from below. However, as $R_{\mathrm{d}} > 0$, a too small value for d is disastrous for the transmit array gain. On the other hand, there is an optimum separation d_{opt} for which the transmit array gain is maximum. From Fig. 11, d_{opt} is always less than half the wavelength. Because $\lambda/2$-spaced isotropic antennas are uncoupled [see (50)], we can conclude that *with the correct antenna spacing, the antenna mutual coupling always improves the transmit array gain compared with uncoupled antennas, regardless of how lossy the antennas are*.

Note from Fig. 11 that, for $R_{\mathrm{d}}/R_{\mathrm{r}} \leq 10^{-2}$, one can achieve with $N = 4$ antennas a transmit array gain $A_{\mathrm{Tx}} > 10$, provided one uses the optimum antenna separation and applies the optimum beamforming vector (see Section VI-B).

The optimum antenna separation depends on the direction of beamforming, number of antennas, and the ratio $R_{\mathrm{d}}/R_{\mathrm{r}}$. Fig. 12 shows the results for the end-fire direction and a uniform linear array of isotropic radiators, e.g., with $N = 4$ antennas which have $R_{\mathrm{d}} = 10^{-3} \times R_{\mathrm{r}}$, we have $d_{\mathrm{opt}} \approx 0.21\lambda$. However, $N = 8$ antennas with an $R_{\mathrm{d}} = 10^{-2} \times R_{\mathrm{r}}$ need a little bit more room to breathe. They are most happy with 0.37λ space between neighbors. Note from Fig. 12 that the more antennas we have, or the more lossy they are, the more close d_{opt} comes to $\lambda/2$.

B. Array Efficiency

Recall from Section IV-A that the transmit impedance matching strategy has no impact on the transmit array gain. Hence, we can choose any matching strategy we like. For mathematical convenience, let us use power matching as defined in (103). A generator voltage envelope vector $\boldsymbol{v}_{\mathrm{G}}$ then lets electric currents flow through the antennas according to

$$\boldsymbol{i}_{\mathrm{A}} = \frac{-\mathrm{j}}{2\sqrt{RR_{\mathrm{r}}}} \left(\boldsymbol{C}_{\mathrm{T}} + \frac{R_{\mathrm{d}}}{R_{\mathrm{r}}}\mathbf{I}_N\right)^{-1/2} \boldsymbol{v}_{\mathrm{G}} \tag{113}$$

which is easily verified by the elementary analysis of the circuit in Fig. 2. The power that is dissipated in the antenna array is then given by

$$P_{\mathrm{d}} = R_{\mathrm{d}}\mathrm{E}\left[\|\boldsymbol{i}_{\mathrm{A}}\|_2^2\right] \tag{114}$$

$$= \frac{R_{\mathrm{d}}}{4RR_{\mathrm{r}}}\mathrm{E}\left[\boldsymbol{v}_{\mathrm{G}}^{\mathrm{H}}\left(\boldsymbol{C}_{\mathrm{T}} + \frac{R_{\mathrm{d}}}{R_{\mathrm{r}}}\mathbf{I}_N\right)^{-1}\boldsymbol{v}_{\mathrm{G}}\right]. \tag{114a}$$

From (63), the optimum vector of generator voltage envelopes is given by

$$\boldsymbol{v}_{\mathrm{G,opt}} = \zeta \cdot v_{\mathrm{G}} \cdot \left(\boldsymbol{C}_{\mathrm{T}} + \frac{R_{\mathrm{d}}}{R_{\mathrm{r}}}\mathbf{I}_N\right)^{-1/2} \boldsymbol{a}_{\mathrm{T}}^{*} \tag{115}$$

where $v_{\mathrm{G}} \in \mathbb{C} \cdot V$ is the information carrying signal which we want to transfer to the receiver and ζ is a constant. Because of power matching, we have $\boldsymbol{B} = \mathbf{I}_N$, and it follows from (23) and (115), setting $\boldsymbol{v}_{\mathrm{G}} = \boldsymbol{v}_{\mathrm{G,opt}}$ that

$$P_{\mathrm{Tx}} = \frac{|\zeta|^2\mathrm{E}\left[|v_{\mathrm{G}}|^2\right]}{4R}\boldsymbol{a}_{\mathrm{T}}^{\mathrm{T}}\left(\boldsymbol{C}_{\mathrm{T}} + \frac{R_{\mathrm{d}}}{R_{\mathrm{r}}}\mathbf{I}_N\right)^{-1}\boldsymbol{a}_{\mathrm{T}}^{*}. \tag{116}$$

Substituting (115) for $\boldsymbol{v}_{\mathrm{G}}$ in (114a), the dissipated power can be written with the help of (116) as

$$P_{\mathrm{d}} = P_{\mathrm{Tx}}\frac{R_{\mathrm{d}}}{R_{\mathrm{r}}}\frac{\boldsymbol{a}_{\mathrm{T}}^{\mathrm{T}}\left(\boldsymbol{C}_{\mathrm{T}} + \frac{R_{\mathrm{d}}}{R_{\mathrm{r}}}\mathbf{I}_N\right)^{-2}\boldsymbol{a}_{\mathrm{T}}^{*}}{\boldsymbol{a}_{\mathrm{T}}^{\mathrm{T}}\left(\boldsymbol{C}_{\mathrm{T}} + \frac{R_{\mathrm{d}}}{R_{\mathrm{r}}}\mathbf{I}_N\right)^{-1}\boldsymbol{a}_{\mathrm{T}}^{*}}. \tag{117}$$

The array efficiency is then defined as

$$\eta_{\mathrm{A}} = \frac{P_{\mathrm{rad}}}{P_{\mathrm{rad}} + P_{\mathrm{d}}} = \frac{P_{\mathrm{rad}}}{P_{\mathrm{Tx}}} = \frac{P_{\mathrm{Tx}} - P_{\mathrm{d}}}{P_{\mathrm{Tx}}} \tag{118}$$

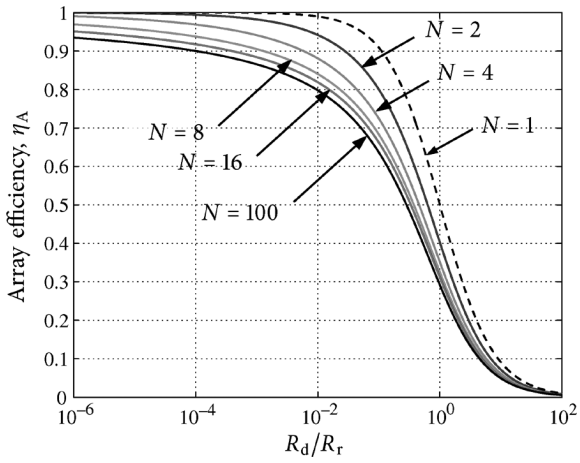

Fig. 13. Array efficiency as a function of R_d/R_r for a different number of antennas. Beamforming is done in the end-fire direction.

which is the ratio of radiated power to the total power supplied into the antenna array. With (117), we obtain

$$\eta_A = 1 - \frac{R_d}{R_r}\frac{\boldsymbol{a}_T^H\left(\boldsymbol{C}_T + \frac{R_d}{R_r}\mathbf{I}_N\right)^{-2}\boldsymbol{a}_T}{\boldsymbol{a}_T^H\left(\boldsymbol{C}_T + \frac{R_d}{R_r}\mathbf{I}_N\right)^{-1}\boldsymbol{a}_T} \tag{119}$$

where $P_d = P_d^*$ is used. In Fig. 13, the array efficiency of a uniform linear array of lossy isotropic antennas is shown, which is employed for beamforming in the end-fire direction. The distance between antennas is chosen such as to maximize the array gain (see Fig. 12). The array efficiency depends only very little on the number of antennas. It mostly depends on the ratio R_d/R_r. From Fig. 13, we can observe that the array efficiency is actually quite high, provided that the optimum antenna separation is chosen and the optimum excitation (115) is used. For $10^{-4} < R_d/R_r < 10^{-2}$, the array efficiency ranges between 80% and 99.5%. For example, with $N = 4$ and $R_d/R_r = 10^{-3}$, we can see from Fig. 11 and Fig. 13 that a transmit array gain of $A_{Tx} \approx 13$ can be achieved with an efficiency of $\eta_A \approx 94\%$, provided that $d = d_{opt} \approx 0.21\lambda$. That surely is a good performance for a lossy four-element array with 0.63λ aperture. Notice, too, that $A_{Tx} = 13$ is less than 1 dB away from the theoretical maximum of 16 but more than 5 dB larger than the number of antennas.

C. Bad Efficiency Reputation

Ever since the frequently cited work by Yaru [14], densely packed antenna arrays have gotten a bad reputation for being grossly inefficient, easily having efficiencies as low as 10^{-14} or even worse. How does this combine with our result from Section VI-B where the efficiency of dense arrays is shown to be quite high (see Fig. 13)?

In order to understand this, it is helpful to realize that, in [14], many antennas are placed extremely close together, like $d = \lambda/64 \approx 0.016\lambda$. We know by now from Fig. 12 that this is far too close for a nonsupraconducting antenna. Moreover, [14] does not use optimized antenna excitation (beamforming) which would take the antenna losses into account [like (115)].

Of course, it is not too difficult an exercise to obtain similar results as in [14] when less than optimum beamforming is used and the antennas are spaced very closely together (for example, $d = \lambda/64$). To demonstrate this, we choose to use a beamforming which is optimized for a *lossless* array. From (113) and (115), the optimum array current vector for the case $R_d = 0$ equals

$$\boldsymbol{i}_A = \frac{-j\zeta v_G}{2\sqrt{RR_r}}\boldsymbol{C}_T^{-1}\boldsymbol{a}_T^*.$$

In order to get this current excitation with the lossy array and its power matching network, we set up the generators as

$$\boldsymbol{v}_G = \zeta \cdot v_G \cdot \left(\boldsymbol{C}_T + \frac{R_d}{R_r}\mathbf{I}_N\right)^{1/2}\boldsymbol{C}_T^{-1}\boldsymbol{a}_T^*.$$

By following the same line of argument as in Section VI-B, we obtain for the array efficiency

$$\eta_A' = 1 - \frac{R_d}{R_r}\frac{\boldsymbol{a}_T^H\boldsymbol{C}_T^{-2}\boldsymbol{a}_T}{\boldsymbol{a}_T^H\boldsymbol{C}_T^{-1}\left(\boldsymbol{C}_T + \frac{R_d}{R_r}\mathbf{I}_N\right)\boldsymbol{C}_T^{-1}\boldsymbol{a}_T}.$$

Suppose $N = 5$, $d = \lambda/64$, and $R_d/R_r = 10^{-3}$. For beamforming in the end-fire direction, we obtain an $\eta_A' \approx 2 \times 10^{-9}$. Radiating 1 W of power requires dissipating 1/2 GW of power in the antenna. Of course, such high dissipation is completely impractical. Hence, the array could radiate only very little power. This is the main argument of [14].

However, note that $d = \lambda/64 \approx 0.016\lambda$ is much too dense. If the optimum separation $d_{opt} \approx 0.255\lambda$ is used instead and the optimum excitation is applied, the efficiency instantly climbs up to $\eta_A \approx 93\%$. To radiate 1 W of power, the array now dissipates only 78 mW, which is reasonable. The transmit array gain for $R_d/R_r = 10^{-3}$ equals $A_{Tx} \approx 18$, which is less than 1.5 dB away from the maximum of 25 and more than 5.5 dB larger than the number of antennas. This array has an aperture of just a little more than one wavelength. *Therefore, to extract the potentially high gain of compact antenna arrays, it is crucial to choose the antenna separation carefully, such that high array efficiency can be retained.*

VII. Conclusion and Outlook

"Did we get the physics right in the modeling of multichannel communication systems?" This question was the starting point of the investigations reported in this paper which have lead to quite a number of interesting insights and results. A multi-antenna radio communications system has to be modeled by linear multiports to enable consistency with the underlying physics. As shown, the computation of transmit power or receiver noise covariance requires knowledge of the governing physics. Circuit theory is shown to be the perfect link to bridge the gap between electromagnetic theory, information theory, and signal processing. The main contributions are as follows.

1) A linear multiport model of antenna-array-based communication systems is derived using only simple far-field calculations of the electromagnetic field and its power density based on energy conversation in lossless media.

2) Array gain is defined as the enhancement of SNR compared with a single-antenna configuration. This results, in general, in different transmit and receive array gains despite the fact that antennas themselves are reciprocal.
3) Transmit array gain does not depend on which strategy of transmit impedance matching is used, although it definitely makes sense to apply power matching to exploit the available power from the high-power transmit amplifiers. This is also advantageous from the viewpoint of sensitivity with respect to the components of the matching network and its source and load.
4) Receive array gain depends on the receiver's impedance matching network and on the properties of the extrinsic (received via the antennas) and intrinsic noise (originating from the low-noise receive amplifiers and subsequent circuitry).
5) The optimum strategy for the receive impedance matching is the decoupling of antenna elements with noise matching. If extrinsic and intrinsic noises have the same covariance matrix, then transmit and receive array gains are identical and maximum in the end-fire direction, where they grow with the square of the number of array elements as the distance between elements becomes small (less than half of the wavelength).
6) If, instead of decoupling and noise matching, the receive matching network merely cancels out the imaginary part of the array's impedance matrix, the receive array gain can even increase exponentially with the number of the antenna elements, provided that the inter-element spacing is less than half of the wavelength.
7) For MIMO systems (where antenna arrays are employed at both ends of the radio link), power matching should be used on the transmit side and noise matching should be used on the receive side. The channel matrix used in the information theoretic context can be computed from the multiport models derived in this paper. This channel matrix can have a full rank, henceforth supporting multistream transmission even if the antennas are densely spaced.
8) Losses in the antenna elements lead to a graceful degradation of the efficiency if taken into account at the design stage, i.e., if the antenna spacing and the beamforming are optimized, accounting for this effect.

The results and insights presented here open up a number of new research directions such as the following:

1) optimized design of antenna elements and arrays for MIMO systems;
2) optimal design of realizable impedance matching multiports taking into account the system bandwidth (broadband matching [44]);
3) optimizing sensitivity of such systems to variations in parameter values;
4) considering multiuser/multicell scenarios, and making the numerous important information theoretic results consistent with the physics of communications.

This can be summarized as not only trying to achieve capacity for a *given* MIMO communication channel but also to *design the channel* for optimum capacity. Circuit theory is the mediator between physics and information theory on the way toward this ambitious goal.

APPENDIX A
ON THE VALIDITY OF THE UNILATERAL APPROXIMATION

Using the following impedance matching:

$$\boldsymbol{Z}_{\mathrm{MT}} = \begin{bmatrix} \mathbf{O} & \mathrm{j}\left(R\mathrm{Re}\{\boldsymbol{Z}_{\mathrm{AT}}\}\right)^{1/2} \\ \mathrm{j}\left(R\mathrm{Re}\{\boldsymbol{Z}_{\mathrm{AT}}\}\right)^{1/2} & -\mathrm{j}\mathrm{Im}\{\boldsymbol{Z}_{\mathrm{AT}}\} \end{bmatrix}$$
$$\boldsymbol{Z}_{\mathrm{MR}} = \begin{bmatrix} \mathbf{O} & -\mathrm{j}\left(R\mathrm{Re}\{\boldsymbol{Z}_{\mathrm{AR}}\}\right)^{1/2} \\ -\mathrm{j}\left(R\mathrm{Re}\{\boldsymbol{Z}_{\mathrm{AR}}\}\right)^{1/2} & -\mathrm{j}\mathrm{Im}\{\boldsymbol{Z}_{\mathrm{AR}}\} \end{bmatrix}$$

we obtain for the noise-free case ($\tilde{\boldsymbol{v}}_{\mathrm{N}} = \mathbf{0}$ and $\boldsymbol{v}_{\mathrm{B}} = \boldsymbol{v}_{\mathrm{C}}$)

$$\begin{bmatrix} \boldsymbol{v}_{\mathrm{T}} \\ \boldsymbol{v}_{\mathrm{R}} \end{bmatrix} = \begin{bmatrix} \boldsymbol{Z}_{\mathrm{T}} & \boldsymbol{Z}_{\mathrm{TR}} \\ \boldsymbol{Z}_{\mathrm{RT}} & \boldsymbol{Z}_{\mathrm{R}} \end{bmatrix} \begin{bmatrix} \boldsymbol{i}_{\mathrm{T}} \\ \boldsymbol{i}_{\mathrm{R}} \end{bmatrix} \tag{120}$$

by using the unilateral approximation (13), where $\boldsymbol{Z}_{\mathrm{T}} = R\mathbf{I}$, $\boldsymbol{Z}_{\mathrm{R}} = R\mathbf{I}$, and $\boldsymbol{Z}_{\mathrm{RT}} = R(\mathrm{Re}\{\boldsymbol{Z}_{\mathrm{AR}}\})^{-1/2}\boldsymbol{Z}_{\mathrm{ART}}(\mathrm{Re}\{\boldsymbol{Z}_{\mathrm{AT}}\})^{-1/2}$, while $\boldsymbol{Z}_{\mathrm{TR}} = \mathbf{O}$. Of course, this leads to the following simple relationship:

$$\boldsymbol{v}_{\mathrm{T}} \approx R\boldsymbol{i}_{\mathrm{T}}. \tag{121}$$

Because we do know that the impedance matrix from (120) is, in fact, symmetric, we obtain another approximation when we set $\boldsymbol{Z}_{\mathrm{TR}} = \boldsymbol{Z}_{\mathrm{RT}}^{\mathrm{T}} = R(\mathrm{Re}\{\boldsymbol{Z}_{\mathrm{AT}}\})^{-1/2}\boldsymbol{Z}_{\mathrm{ART}}^{\mathrm{T}}(\mathrm{Re}\{\boldsymbol{Z}_{\mathrm{AR}}\})^{-1/2}$. It still is an approximation, since the given value for $\boldsymbol{Z}_{\mathrm{RT}}$ is the one obtained from the unilateral approximation. However, suppose that $\|\boldsymbol{Z}_{\mathrm{ART}}\|_{\mathrm{F}}$ is very small, such that the unilateral approximation is almost exact. Then, the given value for $\boldsymbol{Z}_{\mathrm{RT}}$ is almost exact, too. Hence, in the noise-free case ($\boldsymbol{v}_{\mathrm{R}} = -R\boldsymbol{i}_{\mathrm{R}}$; see Fig. 2), the following result:

$$\boldsymbol{v}_{\mathrm{T}} \approx R\left(\mathbf{I} - \frac{1}{2R^2}\boldsymbol{Z}_{\mathrm{RT}}^{\mathrm{T}}\boldsymbol{Z}_{\mathrm{RT}}\right)\boldsymbol{i}_{\mathrm{T}} \tag{122}$$

is almost exact, provided that $\|\boldsymbol{Z}_{\mathrm{ART}}\|_{\mathrm{F}}$ is sufficiently small. In order to find out how small it actually has to be, we can compare the result (122) to the result (121). Since the latter is exact for $\|\boldsymbol{Z}_{\mathrm{ART}}\|_{\mathrm{F}} = 0$, we conclude that $\|\boldsymbol{Z}_{\mathrm{ATR}}\|_{\mathrm{F}}$ is sufficiently small when the difference between both results is negligible. Let us define the symbol Θ as the event when $\|\boldsymbol{Z}_{\mathrm{ART}}\|_{\mathrm{F}}$ is sufficiently small. Then, from comparing (122) and (121)

$$\left\|\frac{1}{2R^2}\boldsymbol{Z}_{\mathrm{RT}}^{\mathrm{T}}\boldsymbol{Z}_{\mathrm{RT}}\right\|_{\mathrm{F}} \ll \|\mathbf{I}_N\|_{\mathrm{F}} \Longrightarrow \Theta. \tag{123}$$

Because $\|\boldsymbol{Z}_{\mathrm{RT}}^{\mathrm{T}}\boldsymbol{Z}_{\mathrm{RT}}\|_{\mathrm{F}} \leq \|\boldsymbol{Z}_{\mathrm{RT}}^{\mathrm{T}}\|_{\mathrm{F}} \cdot \|\boldsymbol{Z}_{\mathrm{RT}}\|_{\mathrm{F}} = \|\boldsymbol{Z}_{\mathrm{RT}}\|_{\mathrm{F}}^2$ and, furthermore, $\|\mathbf{I}_N\|_{\mathrm{F}} = N^{1/2} \geq 1$, it follows that

$$\|\boldsymbol{Z}_{\mathrm{RT}}\|_{\mathrm{F}} \ll R \Longrightarrow \Theta. \tag{124}$$

With $\boldsymbol{Z}_{\mathrm{RT}} = R(\mathrm{Re}\{\boldsymbol{Z}_{\mathrm{AR}}\})^{-1/2}\boldsymbol{Z}_{\mathrm{ART}}(\mathrm{Re}\{\boldsymbol{Z}_{\mathrm{AT}}\})^{-1/2}$, we have

$$\|\boldsymbol{Z}_{\mathrm{RT}}\|_{\mathrm{F}} \leq R \cdot \|\boldsymbol{Z}_{\mathrm{ART}}\|_{\mathrm{F}} \cdot \left\|\mathrm{Re}\{\boldsymbol{Z}_{\mathrm{AR}}\}^{-1/2}\right\|_{\mathrm{F}} \cdot \left\|\mathrm{Re}\{\boldsymbol{Z}_{\mathrm{AT}}\}^{-1/2}\right\|_{\mathrm{F}}$$

such that, with (124)

$$\|\boldsymbol{Z}_{\mathrm{ART}}\|_{\mathrm{F}} \ll \frac{1}{\left\|\mathrm{Re}\{\boldsymbol{Z}_{\mathrm{AR}}\}^{-1/2}\right\|_{\mathrm{F}} \cdot \left\|\mathrm{Re}\{\boldsymbol{Z}_{\mathrm{AT}}\}^{-1/2}\right\|_{\mathrm{F}}} \Longrightarrow \Theta. \tag{125}$$

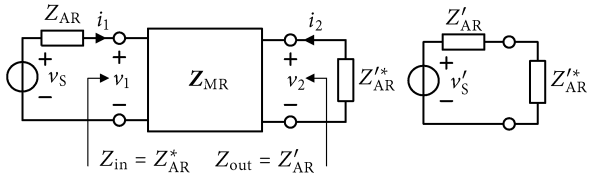

Fig. 14. (Left) Generator connected to lossless twoport terminated with the complex conjugate match. (Right) Equivalent circuit.

Now, there is

$$\left\|\mathrm{Re}\{\boldsymbol{Z}_{\mathrm{AT}}\}^{-1/2}\right\|_{\mathrm{F}}=\sqrt{\mathrm{tr}\left(\mathrm{Re}\{\boldsymbol{Z}_{\mathrm{AT}}\}^{-1}\right)}=\sqrt{\sum_{n=1}^{N}\frac{1}{\xi_n}}\leq\sqrt{\frac{N}{\xi}}$$

where ξ_n denotes the eigenvalues of $\mathrm{Re}\{\boldsymbol{Z}_{\mathrm{AT}}\}$ and ξ is the *smallest* eigenvalue. Similarly, we have

$$\left\|\mathrm{Re}\{\boldsymbol{Z}_{\mathrm{AR}}\}^{-1/2}\right\|_{\mathrm{F}}=\sqrt{\mathrm{tr}\left(\mathrm{Re}\{\boldsymbol{Z}_{\mathrm{AR}}\}^{-1}\right)}=\sqrt{\sum_{m=1}^{M}\frac{1}{\xi'_m}}\leq\sqrt{\frac{M}{\xi'}}$$

where ξ'_n are the eigenvalues of $\mathrm{Re}\{\boldsymbol{Z}_{\mathrm{AR}}\}$ and ξ' is the *smallest* eigenvalue. With (125), it therefore follows that

$$\|\boldsymbol{Z}_{\mathrm{ART}}\|_{\mathrm{F}}\ll\sqrt{\frac{\xi\xi'}{MN}}\Longrightarrow\Theta. \tag{126}$$

Appendix B
Voltage Transformation

In the upper part of the circuit in Fig. 9, temporarily disconnect the noisy amplifier from the matching network and terminate the latter with the complex conjugate of its output impedance, as displayed on the left-hand side of Fig. 14. Describing the lossless matching twoport by

$$\begin{bmatrix}v_1\\v_2\end{bmatrix}=\mathrm{j}\begin{bmatrix}a&b\\b&c\end{bmatrix}\begin{bmatrix}i_1\\i_2\end{bmatrix}$$

where $a,b,c\in\mathbb{R}\cdot\Omega$ are arbitrary *real* resistance values, with $b\neq 0$, then the output impedance equals

$$Z'_{\mathrm{AR}}=\mathrm{j}c+\frac{b^2}{Z_{\mathrm{AR}}+\mathrm{j}a}. \tag{127}$$

The input impedance (i.e., the load impedance seen by the generator) is similarly given by

$$Z_{\mathrm{in}}=\mathrm{j}a+\frac{b^2}{Z'^{*}_{\mathrm{AR}}+\mathrm{j}c}. \tag{128}$$

Substituting (127) in (128) reveals that $Z_{\mathrm{in}}=Z^{*}_{\mathrm{AR}}$, i.e., we have a complex conjugated match. Hence, the active power delivered by the generator is given by $P_{\mathrm{G}}=(1/4)\mathrm{E}[|v_{\mathrm{S}}|^2]/\mathrm{Re}\{Z_{\mathrm{AR}}\}$. The equivalent circuit from the right-hand side of Fig. 14 shows that the active power which is delivered into the load equals $P_{\mathrm{L}}=(1/4)\mathrm{E}[|v'_{\mathrm{S}}|^2]/\mathrm{Re}\{Z'_{\mathrm{AR}}\}$. As the impedance matching network is lossless, we have $P_{\mathrm{G}}=P_{\mathrm{L}}$, and therefore

$$\mathrm{E}\left[\left|v'_{\mathrm{S}}\right|^2\right]=\mathrm{E}\left[|v_{\mathrm{S}}|^2\right]\cdot\frac{\mathrm{Re}\left\{Z'_{\mathrm{AR}}\right\}}{\mathrm{Re}\{Z_{\mathrm{AR}}\}}.$$

Appendix C
Derivation of Equation (90)

From (27), the first line of (20), and (51), we have

$$\boldsymbol{\Upsilon}=\frac{2R_{\mathrm{N}}^2}{R_{\mathrm{r}}^2}\left(1-\frac{\mathrm{Re}\{\rho^*Z_{\mathrm{opt}}\}}{R_{\mathrm{N}}}\right)\mathbf{I}_M+\frac{\tilde{\beta}\mathrm{Re}\{Z_{\mathrm{opt}}\}}{\beta R_{\mathrm{r}}}\boldsymbol{C}_{\mathrm{R}}^{-1/2}\boldsymbol{\phi}\boldsymbol{C}_{\mathrm{R}}^{-1/2} \tag{129}$$

where we have also used the $|Z_{\mathrm{opt}}|=R_{\mathrm{N}}$ from (81). Moreover, we find from (81) that

$$\mathrm{Re}\{\rho^*Z_{\mathrm{opt}}\}=R_{\mathrm{N}}\left(\mathrm{Re}\{\rho\}\sqrt{1-(\mathrm{Im}\{\rho\})^2}+(\mathrm{Im}\{\rho\})^2\right)$$

such that (129) can be written as

$$\boldsymbol{\Upsilon}=\sqrt{1-(\mathrm{Im}\{\rho\})^2}\times\left(\frac{2R_{\mathrm{N}}^2}{R_{\mathrm{r}}^2}\left(\sqrt{1-(\mathrm{Im}\{\rho\})^2}-\mathrm{Re}\{\rho\}\right)\mathbf{I}_M+\boldsymbol{\Xi}\right) \tag{130}$$

where

$$\boldsymbol{\Xi}=\frac{\tilde{\beta}R_{\mathrm{N}}}{\beta R_{\mathrm{r}}}\boldsymbol{C}_{\mathrm{R}}^{-1/2}\boldsymbol{\phi}\boldsymbol{C}_{\mathrm{R}}^{-1/2}.$$

From (82), we find

$$\sqrt{1-(\mathrm{Im}\{\rho\})^2}-\mathrm{Re}\{\rho\}=(\mathrm{NF}_{\min}-1)\frac{2\mathrm{k}T_{\mathrm{A}}\Delta f}{\beta R_{\mathrm{N}}}$$

such that substituting this in (130) and using (7) yields (90).

Appendix D
Background Noise Covariance Matrix

Imagine that the background radiation originates from a number of single-antenna transmitters located somewhere in space far away from the receiver antenna array. From (56), the vector of the open-circuit voltage envelopes of the receive antennas is proportional to the receive array steering vector $\boldsymbol{a}_{\mathrm{R}}(\theta_{\mathrm{R},k})$ which corresponds to the kth source of background radiation. Hence

$$\tilde{\boldsymbol{v}}_{\mathrm{N}}=\mathrm{const}\sum_k\gamma_k\boldsymbol{a}_{\mathrm{R}}(\theta_{\mathrm{R},k})$$

where the complex coefficients γ_k contain the amplitude and phase of the signal received from the kth source. The covariance matrix is then given by

$$\mathrm{E}\left[\tilde{\boldsymbol{v}}_{\mathrm{N}}\tilde{\boldsymbol{v}}_{\mathrm{N}}^{\mathrm{H}}\right]=\mathrm{E}\left[\mathrm{const}\sum_k\sum_{k'}\gamma_k\gamma_{k'}^*\boldsymbol{a}_k\boldsymbol{a}_{k'}^{\mathrm{H}}\right]$$

where we used the shorthand $\boldsymbol{a}_k$ to denote $\boldsymbol{a}_{\mathrm{R}}(\theta_{R,k})$. Now, it is reasonable that the different sources of background noise are uncorrelated such that $\mathrm{E}[\gamma_k\gamma_{k'}^*]=0$ for $k\neq k'$. Hence

$$\mathrm{E}\left[\tilde{\boldsymbol{v}}_{\mathrm{N}}\tilde{\boldsymbol{v}}_{\mathrm{N}}^{\mathrm{H}}\right]=\mathrm{const}\sum_k\mathrm{E}\left[|\gamma_k|^2\boldsymbol{a}_k\boldsymbol{a}_k^{\mathrm{H}}\right].$$

Now, let the number of sources approach infinity

$$\mathrm{E}\left[\tilde{\boldsymbol{v}}_{\mathrm{N}}\tilde{\boldsymbol{v}}_{\mathrm{N}}^{\mathrm{H}}\right] = \mathrm{const}\int_0^{2\pi}\int_0^{\pi}\mathrm{E}\left[|\gamma|^2\right]\boldsymbol{a}(\theta)\boldsymbol{a}^{\mathrm{H}}(\theta)\mathrm{d}\theta\mathrm{d}\phi \quad (131)$$

where $\mathrm{E}[|\gamma|^2]$ is, in general, a function of θ and ϕ. Also

$$\mathrm{d}P_{\mathrm{N}} = \mathrm{const}\cdot\mathrm{E}\left[|\gamma|^2\right]\mathrm{d}\theta\mathrm{d}\phi$$

is the available power of background noise that arrives from within the directional window that ranges from θ to $\theta + d\theta$ and from ϕ to $\phi + d\phi$. With the density P'_{N} of the available power of the background radiation, we can write this also as $\mathrm{d}P_{\mathrm{N}} = P'_{\mathrm{N}}\mathrm{d}A$, where $\mathrm{d}A = r^2\sin(\theta)\mathrm{d}\theta\mathrm{d}\phi$ denotes the infinitesimal area that corresponds to the directional window. Hence

$$\mathrm{E}\left[|\gamma|^2\right] = \mathrm{const}\cdot P'_{\mathrm{N}}\cdot r^2\sin\theta.$$

When we substitute this into (131), we obtain

$$\mathrm{E}\left[\tilde{\boldsymbol{v}}_{\mathrm{N}}\tilde{\boldsymbol{v}}_{\mathrm{N}}^{\mathrm{H}}\right] = \mathrm{const}\int_0^{2\pi}\int_0^{\pi}P'_{\mathrm{N}}(\theta,\phi)\cdot\boldsymbol{a}(\theta)\boldsymbol{a}^{\mathrm{H}}(\theta)\sin(\theta)\mathrm{d}\theta\mathrm{d}\phi \quad (132)$$

where we have fixed r to a constant value which ensures that the complete antenna array is inside the corresponding sphere around it and all sources of background noise remain outside the sphere. From (5) and (8), the matrix $\boldsymbol{\phi}$ is equal to (132), normalized to unity entries in its main diagonal

$$\boldsymbol{\phi} = \frac{\int_0^{2\pi}\int_0^{\pi}P'_{\mathrm{N}}(\theta,\phi)\cdot\boldsymbol{a}(\theta)\boldsymbol{a}^{\mathrm{H}}(\theta)\sin(\theta)\mathrm{d}\theta\mathrm{d}\phi}{\int_0^{2\pi}\int_0^{\pi}P'_{\mathrm{N}}(\theta,\phi)|a(\theta)|^2\sin(\theta)\mathrm{d}\theta\mathrm{d}\phi} \quad (133)$$

where $|a(\theta)|$ is the magnitude of the entries of the array steering vector $\boldsymbol{a}(\theta)$. For isotropic antennas, $|a(\theta)| = 1$ such that

$$\boldsymbol{\phi} = \frac{\int_0^{2\pi}\int_0^{\pi}P'_{\mathrm{N}}(\theta,\phi)\cdot\boldsymbol{a}(\theta)\boldsymbol{a}^{\mathrm{H}}(\theta)\sin(\theta)\mathrm{d}\theta\mathrm{d}\phi}{\int_0^{2\pi}\int_0^{\pi}P'_{\mathrm{N}}(\theta,\phi)\sin(\theta)\mathrm{d}\theta\mathrm{d}\phi}.$$

If the background radiation is also isotropic, we know that P'_N does not depend on θ, or ϕ, such that

$$\boldsymbol{\Phi}_{\mathrm{iso}} = \frac{1}{2}\int_0^{\pi}\boldsymbol{a}(\theta)\boldsymbol{a}^{\mathrm{H}}(\theta)\sin(\theta)\mathrm{d}\theta = \boldsymbol{C}_{\mathrm{R}} \in \mathbb{R}^{M\times M}$$

where the second equality stems from (44) when it is written for the receive array instead of the transmit array. This shows that $\boldsymbol{\Phi} = \boldsymbol{C}_R$ is the normalized covariance matrix of *isotropic* background radiation. Notice that $\boldsymbol{\Phi}_{\mathrm{iso}}$ is a real-valued $M \times M$ matrix, with unity on its main diagonal.

REFERENCES

[1] A. Fettweis, "Wave digital filters: Theory and practice," *Proc. IEEE*, vol. 74, no. 2, pp. 270–327, Feb. 1986.

[2] I. E. Telatar, "Capacity of multi-antenna Gaussian channels," *Eur. Trans. Telecommun.*, vol. 10, no. 6, pp. 585–596, Nov. 1999.

[3] H. M. Paynter, *Analysis and Design of Engineering Systems*. Cambridge, MA: MIT Press, 1961.

[4] V. Belevitch, "Elementary applications of the scattering formalism to network design," *IRE Trans. Circuit Theory*, vol. 3, no. 2, pp. 97–104, Jun. 1956.

[5] F. K. Gruber and E. A. Marengo, "New aspects of electromagnetic information theory for wireless and antenna systems," *IEEE Trans. Antennas Propag.*, vol. 56, no. 11, pp. 3470–3484, Nov. 2008.

[6] M. D. Migliore, "An intuitive electromagnetic approach to MIMO communication systems," *IEEE Antennas Propag. Mag.*, vol. 48, no. 3, pp. 128–137, Jun. 2006.

[7] J. Y. Hui, C. Bi, and H. Sun, "Spatial communication capacity based on electromagnetic wave equations," in *Proc. IEEE ISIT*, Washington, DC, Jun. 2001, p. 337.

[8] H. Hillbrand and P. Russer, "An efficient method for computer aided noise analysis of linear amplifier networks," *IEEE Trans. Circuits Syst.*, vol. CAS-23, no. 4, pp. 235–238, Apr. 1976.

[9] H. Hillbrand and P. Russer, "Correction to: An efficient method for computer aided noise analysis of linear amplifier networks," *IEEE Trans. Circuits Syst.*, vol. CAS-23, no. 11, pp. 691–691, Nov. 1976.

[10] M. E. Mokari and W. Patience, "A new method of noise parameter calculation using direct matrix analysis," *IEEE Trans. Circuits Syst.*, vol. 39, no. 9, pp. 767–771, Sep. 1992.

[11] F. Principato, G. Ferrante, and R. N. Mantegna, "A method for the analytical calculation of noise parameters of linear two-ports with cross-correlated noise sources," *IEEE Trans. Circuits Syst.*, vol. 46, no. 8, pp. 1019–1022, Aug. 1999.

[12] J. W. Wallace and M. A. Jensen, "Mutual coupling in MIMO wireless systems: A rigorous network theory analysis," *IEEE Trans. Wireless Commun.*, vol. 3, no. 4, pp. 1317–1325, Jul. 2004.

[13] S. A. Schelkunoff, "A mathematical theory of linear arrays," *Bell Syst. Tech. J.*, vol. 22, pp. 80–87, Jan. 1943.

[14] N. Yaru, "A note on super-gain antenna arrays," *Proc. IRE*, vol. 39, no. 9, pp. 1081–1085, Sep. 1951.

[15] K. F. Warnick, E. E. Woestenburg, L. Belostotski, and P. Russer, "Minimizing the noise penalty due to mutual coupling for a receiving array," *IEEE Trans. Antennas Propag.*, vol. 57, no. 6, pp. 1634–1644, Jun. 2009.

[16] H. Nyquist, "Thermal agitation of electric charge in conductor," *Phys. Rev.*, vol. 32, no. 1, pp. 110–113, Jul. 1928.

[17] V. Belevitch, *Classical Network Theory*. San Francisco, CA: Holden Day, 1968.

[18] A. Balanis, *Antenna Theory*, 2nd ed. Hoboken, NJ: Wiley, 1997.

[19] W. Wasylkiwskyj and W. K. Kahn, "Theory of mutual coupling among minimum-scattering antennas," *IEEE Trans. Antennas Propag.*, vol. 18, no. 2, pp. 204–216, Mar. 1970.

[20] K. Kahn and H. Kurss, "Minimum-scattering antennas," *IEEE Trans. Antennas Propag.*, vol. AP-13, no. 5, pp. 671–675, Sep. 1965.

[21] R. S. Bokulić, "Use basic concepts to determine antenna noise temperature," *Microw. RF*, vol. 30, pp. 107–115, Mar. 1991.

[22] S. A. Schelkunoff and H. T. Friis, *Antennas. Theory and Practice*. New York: Wiley, 1952.

[23] D. H. Johnson and D. E. Dudgeon, *Array Signal Processing*. Englewood Cliffs, NJ: Prentice-Hall, 1993.

[24] M. Haardt, *Efficient One-, Two-, and Multidimensional High-Resolution Array Signal Processing*. Aachen, Germany: Shaker Verlag, 1996.

[25] J. C. Liberti and T. S. Rappaport, *Smart Antennas for Wireless Communications*. Englewood Cliffs, NJ: Prentice-Hall, 1999.

[26] D. S. Shiu, G. J. Foschini, M. J. Gans, and J. M. Kahn, "Fading correlation, and its effect on the capacity of multi-element antenna systems," *IEEE Trans. Commun.*, vol. 48, no. 3, pp. 502–512, Mar. 2000.

[27] D. Tse and P. Viswanath, *Fundamentals of Wireless Communication*. Cambridge, U.K.: Cambridge Univ. Press, 2005.

[28] R. P. Feynman, R. B. Leighton, and M. Sands, *The Feynman Lectures on Physics*. Reading, MA: Addison-Wesley, 1963, vol. II.

[29] H. Yordanov, M. T. Ivrlač, P. Russer, and J. A. Nossek, "Arrays of isotropic radiators—A field-theoretic justification," in *Proc. IEEE/ITG Int. Workshop Smart Antennas*, Berlin, Germany, Feb. 2009.

[30] J. D. Jackson, *Classical Electrodynamics*. New York: Wiley, 1998.

[31] M. T. Ivrlač and J. A. Nossek, "The maximum achievable array gain under physical transmit power constraint," in *Proc. IEEE Int. Symp. Inf. Theory Appl.*, Dec. 2008, pp. 1338–1343.

[32] E. E. Altshuler, T. H. O'Donnell, A. D. Yaghjian, and S. R. Best, "A monopole superdirective array," *IEEE Trans. Antennas Propag.*, vol. 53, no. 8, pp. 2653–2661, Aug. 2005.

[33] A. D. Yaghjian, T. H. O'Donnell, E. E. Altshuler, and S. R. Best, "Electrically small supergain end-fire arrays," *Radioscience, Vol. 43,* vol. 43, 2008 [Online]. Available: RS3002,doi:10.1029/2007RS003747

[34] H. T. Friis, "Noise figure of radio receivers," *Proc. IRE*, vol. 32, no. 7, pp. 419–422, Jul. 1944.

[35] K. F. Warnick and M. A. Jensen, "Optimal noise matching for mutually coupled arrays," *IEEE Trans. Antennas Propag.*, vol. 55, no. 6, pp. 1726–1731, Jun. 2007.
[36] C. E. Shannon, "A mathematical theory of communications," *Bell Syst. Tech. J.*, vol. 27, pp. 379–423, Jul. 1948, 623–656.
[37] G. J. Foschini and M. J. Gans, "On limits of wireless communications in a fading environment using multiple antennas," *Wireless Pers. Commun.*, vol. 6, no. 3, pp. 311–335, Mar. 1998.
[38] S. Vishwanath, N. Jindal, and A. Goldsmith, "On the capacity of multiple input multiple output broadcast channels," *IEEE Trans. Inf. Theory*, vol. 49, no. 10, pp. 2658–2668, Oct. 2003.
[39] H. W. Y. Steinberg and S. Shamai, "The capacity region of the Gaussian MIMO broadcast channel," in *Proc. IEEE Int. Symp. Inf. Theory*, 2004, p. 174.
[40] W. Feller, *An Introduction to Probability Theory and Its Applications*, 3rd ed. New York: Wiley, 1968.
[41] L. Gesbert, H. Bölcskei, D. Gore, and A. J. Paulraj, "MIMO wireless channels: Capacity and performance prediction," in *Proc. IEEE GLOBECOM*, San Francisco, CA, Nov. 2000, pp. 1083–1088.
[42] 3GPP, "A Standardized Set of MIMO Radio Propagation Channels," 3GPP TSGR vol. R1-01-1179, 2001.
[43] M. T. Ivrlač and J. A. Nossek, "Physical modeling of communication systems in information theory," in *Proc. IEEE ISIT*, Seoul, South Korea, Jun. 2009, pp. 2179–2183.
[44] J. W. Helto, "A mathematical view of broadband matching," in *Proc. IEEE Int. Conf. Circuits Syst. Theory*, New York, 1978.

Michel T. Ivrlač received the first Dipl.Ing. degree in electrical engineering from Munich University of Applied Sciences, Munich, Germany, in 1994 and the second Dipl.Ing. degree and the Dr.-Ing. degree in electrical engineering and information technology from the Technische Universität München (tum), Munich, in 1998 and 2005, respectively.

He currently holds the position of a Senior Researcher with the Institute for Circuit Theory and Signal Processing, tum, where he is teaching courses on circuit theory and communication. His main research interests are the physics of communications, signal processing for cellular networks, and coding for ultra-high-speed communications.

Josef A. Nossek (S'72–M'74–SM'81–F'93) received the Dipl.Ing. and Dr. techn. degrees in electrical engineering from Vienna University of Technology, Vienna, Austria, in 1974 and 1980, respectively.

He joined SIEMENS AG, Munich, Germany, in 1978, where he was engaged in the design of both passive and active filters for communication systems. In 1978, he became the Supervisor and, in 1980, the Head of a group of laboratories engaged in designing monolithic filters (analog and digital). Since 1982, he has been the Head of a group of laboratories designing digital radio systems with the Transmission Systems Department, SIEMENS AG. In 1984, he was a Visiting Professor at the University of Capetown, Capetown, Africa. From 1987 to 1989, he was the Head of the Radio Systems Design Department, where he was instrumental in introducing high-speedVLSI signal processing into digital microwave radio. Since April 1989, he has been a Professor of circuit theory and design with the Technische Universität München (TUM), Munich, Germany, where he teaches undergraduate and graduate courses in the field of circuit and system theory and leads research on signal processing algorithms in communications, particularly multi-antenna communication systems.

Dr. Nossek was the President Elect, President, and Past President of the IEEE Circuits and Systems Society in 2001, 2002, and 2003, respectively. He was the Vice President of Verband der Elektrotechnik, Elektronik und Informationstechnik e.V. (VDE) 2005 and 2006 and was the President ofVDE in 2007 and 2008. He was the recipient of ITG Best Paper Award in 1988, the Mannesmann Mobilfunk (currently Vodafone) Innovations Award in 1998, and the Award for Excellence in Teaching from the Bavarian Ministry for Science, Research and Art in 1998. From the IEEE Circuits and Systems Society, he received the Golden Jubilee Medal for "Outstanding Contributions to the Society" in 1999 and the Education Award in 2008. He was the recipient of the "Bundesverdienstkreuz am Bande" in 2008. In 2009, he became an elected member of acatech.